

Iron Formations: A Record of Neoproterozoic to Paleoproterozoic Environmental History

K.O. Konhauser¹, N.J. Planavsky², D.S. Hardisty³, T.W. Lyons³, S.V. Lalonde⁴, E. Pecoits¹,
and A. Bekker³

¹Department of Earth & Atmospheric Sciences, University of Alberta, Edmonton, Alberta, T6G 2E3, Canada

²Department of Geology and Geophysics, Yale University, New Haven, Connecticut, 06520, USA

³Department of Earth Sciences, University of California, Riverside, California, 92521, USA

⁴UMR6538 Domaines Océaniques, European Institute for Marine Studies, Technopôle Brest-Iroise, Plouzané, 29280, France

Abstract

Iron formations are chemical archives of Precambrian seawater chemistry. Given that they accumulated onto the seafloor for over two billion years of Earth's history, temporal changes in their composition offer a unique glimpse into the environmental changes that took place during that time interval. Perhaps one of the most significant events was the transition from an anoxic planet to one where oxygen was persistently present within the marine water column and atmosphere. Linked to this progressive global oxygenation was the evolution of aerobic microbial metabolisms that fundamentally influenced continental weathering processes, the supply of nutrients to the oceans, and, ultimately, diversification of the biosphere to produce complex life forms, such as ourselves. This chapter reviews what iron formations are, and how they have been used to gain insights into the processes underpinning the global rise in oxygen.

1. Introduction

Iron formations are iron-rich (15-40 wt%) and siliceous (40-60 wt%) sedimentary deposits that precipitated from seawater throughout much of the Neoproterozoic and Paleoproterozoic (2.60–1.85 Ga) (James, 1954; Trendall, 2002; Klein, 2005; Bekker et al., 2010). They typically contain low concentrations of Al_2O_3 (<1 wt%) and incompatible elements (Ti, Zr, Th, Hf and Sc <20 ppm), which indicates minimal detrital input to the depositional basin during their deposition, although this does not hold true for all iron formations. They are also characterized by layers of variable thickness, from macrobands (meters in thickness) to the characteristic mesobands (centimeter-thick units) by which they are typically defined (i.e., banded iron formation, BIF), to millimeter and submillimeter layers. The latter are known as microbands and are linked to either periodic hydrothermal or diagenetic processes (e.g., Trendall and Blockley, 1970; Morris, 1993; Krapež et al., 2003). Granular iron formations (GIF) typically lack banding and are made of granules of chert and iron oxides or silicates with early diagenetic chert cement filling pore space (e.g., Simonson, 1985). GIF first appear in the rock record at ca. 2.32 Ga, reach their acme at ca. 1.88 Ga, and are then replaced by ironstones in the Phanerozoic record (after 543 Ma).

The mineralogy of iron formations from the best-preserved successions is remarkably uniform, comprising mostly quartz (in the form of chert), magnetite, hematite, Fe-rich silicate minerals (stilpnomelane, minnesotaite, greenalite, and riebeckite), carbonate minerals (siderite, ankerite, calcite, and dolomite), and minor sulfides (pyrite and pyrrhotite); the presence of both ferric and ferrous minerals gives iron formations an average oxidation state of $\text{Fe}^{2.4+}$ (Klein and Beukes, 1992). James (1954) defined four facies of iron formation: silicate, carbonate, oxide, and sulfide. Sulfide-facies iron formations are pyritic carbonaceous shales and slates and, as such, should no longer be considered iron formation in the strict sense. The other iron formation facies are generally interbedded with variably recrystallised chert (Simonson, 2003). The oxide facies consists

predominantly of magnetite or hematite, whereas carbonate-facies varieties contain siderite or ankerite as major constituents. The mineralogy of silicate-facies iron formations is more complex and depends to a large extent on the degree of metamorphism. Under relatively low-grade metamorphic conditions of the biotite zone and below, greenalite, minnesotaite, stilpnomelane, chamosite and ripidolite (Fe-chlorites), riebeckite, and ferriannite may be present. At higher grades, cummingtonite, grunerite, pyroxene, garnet, and fayalite can occur.

It is generally agreed that none of the minerals in iron formation are primary in origin. Instead, the minerals reflect significant post-depositional alteration under diagenetic and metamorphic conditions (including, in some cases, post-depositional fluid flow). The effect of increasing temperature and pressure is manifested by the progressive change in mineralogy through replacement and recrystallisation, increase in crystal size and obliteration of primary textures (Klein, 2005). For instance, the alternating layers of magnetite and hematite are interpreted to have formed from an initial iron oxyhydroxide phase, e.g., ferrihydrite ($\text{Fe}(\text{OH})_3$), that precipitated in the photic zone when dissolved ferrous iron (at concentrations that may have ranged from 0.03 to 0.5 mM; Holland, 1973; Morris, 1993) was oxidised and hydrolysed to insoluble ferric iron. The iron oxyhydroxide particles then sank through the water column and were deposited on the seafloor where they eventually formed (1) magnetite or iron carbonates when organic remineralisation was coupled with Fe(III) reduction, either during diagenesis or metamorphism; (2) hematite, when organic material was lacking; or (3) iron silicates, possibly in the form of a precursor mineral such as greenalite ($(\text{Fe})_3\text{Si}_2\text{O}_5(\text{OH})_4$), when silica-sorbed ferric oxyhydroxides reacted with other cationic species in the sediment pore waters (Morris, 1993). Ferrous iron sorption to those particles may also have given rise to 'green rust'-type deposits that eventually transformed into magnetite (Tamura et al., 1984; Zegeye et al., 2012), although magnetite textures indicate a predominately metamorphic origin. Organic material, whether in the form of pelagic rain or intimately associated with sinking

iron oxyhydroxide particles, would have fuelled the organic remineralisation reactions mentioned above, and is likely to have been largely consumed by excess Fe oxidants during diagenesis (see section 2.4). Although siderite in IF has been interpreted to be a primary mineral phase (e.g., Beukes and Klein, 1990), there are strong isotopic and petrographic arguments (e.g., Fischer et al., 2009; Johnson et al., 2003, 2008; Pecoits et al., 2009; Heimann et al., 2010) that point instead to formation linked to remineralisation of organic matter. The chert is widely considered to have precipitated from the water column or in pore-waters as colloidal silica co-precipitated with iron-rich particles given that the Archean ocean had significantly elevated concentrations of dissolved silica, at least as high as at saturation with cristobalite (0.67 mM at 40°C in seawater), and possibly even amorphous silica (2.20 mM) (Siever, 1992; Maliva et al., 2005; Konhauser et al., 2007a). An alternative interpretation is that most of the chert formed at the sediment-water interface as a replacement phase of a precursor sediment (Krapež et al., 2003).

Iron formations are broadly defined as being either Superior-type or Algoma-type (Gross, 1980), although it is more suitable to consider these classifications as end members with a gradation of varieties existing (Bekker et al., 2010, 2012). Algoma-type are interlayered with, or stratigraphically and genetically linked to, submarine-emplaced mafic to felsic volcanic rocks and associated volcanoclastic greywackes and shales in greenstone belts, and in many cases, spatially coupled with volcanogenic massive sulfide (VMS) deposits. They were apparently formed close to volcanic arcs and spreading centres and produced by exhalative hydrothermal processes related to volcanism (e.g., Goodwin, 1962). These iron formations contain oxide, silicate and carbonate facies and commonly grade into sulfidic sediments, which can be enriched in copper, zinc, lead, silver, and gold. The lack of any sedimentological features besides fine banding (i.e., absence of current-, tide-, or wave-generated sedimentary structures) in the Algoma-type iron formations indicates a deep-water environment, likely distal to continental landmass (Bekker et al., 2010). In this regard,

Algoma-type iron formations have compositions that reflect local volcanic and hydrothermal conditions. Iron formations precipitated before 3.0 Ga are generally described as being Algoma-type.

In contrast, Superior-type iron formations developed in passive-margin sedimentary successions (i.e., after stable continental shelves evolved) and generally lack direct relations with volcanic rocks. They are regarded as having been deposited in near-shore shelf environments (e.g., Trendall, 2002) because they are typically interbedded with, or grade into, carbonates and black shales (Bekker et al., 2010). Unlike most Algoma-type iron formations, which rarely extend for more than 10 km along strike and are usually not more than 50 m thick, the Superior-type iron formations can be extremely laterally extensive, with original aerial extents estimated in some cases to be over 100,000 km² (Isley, 1995). In terms of mass, the largest Superior-type iron formations contain over 10¹³ tons of iron (Isley, 1995).

Texturally, IF are divided into two groups. BIF are dominant in Eoarchean to early Paleoproterozoic successions. They consist predominantly of interbanded iron- and silica-rich layers and were generally, but not universally, deposited in relatively deep-water settings, as they typically lack evidence for wave or storm action (Simonson and Hassler, 1996; Trendall, 2002; Krapež et al., 2003) (Figure 1A). Most BIF are commonly either overlain or underlain by organic matter-rich and sulfidic shales, and, in some cases, are interstratified with them. For example, the well-studied ~180 meter thick Dales Gorge member of the Brockman IF is comprised of 17 BIF macrobands intercalated with 16 shale (“S”) macrobands (Trendall and Blockley, 1970) (Figure 1B). These shales are thought to be shallower-water equivalents of BIF (e.g., Beukes and Klein, 1990; Beukes et al., 1990; Beukes and Cairncross, 1991; Bau and Dulski, 1996). There are, however, several key examples of shallow-water Archean BIF that are interbedded with sandstones (e.g., Fralick and Pufahl, 2006). Rather counter-intuitively, given evidence for shallow-water anoxia in the Archean,

GIF that formed in high-energy environments are much more common in Paleoproterozoic successions (Figure 1C). GIF are characterised by granules that can vary in morphology, size (micrometers to centimetre in diameter), and composition (chert, iron oxides, iron carbonates, and/or iron silicates); the cement is typically chert (Figure 1D). Many of the granules are considered detrital, with some being derived by sedimentary re-working of iron-rich clays, mudstone, arenites, and even stromatolites (e.g., Ojakangas, 1983; Simonson and Goode, 1989). Others, such as the ca. 2.32 Ga oolitic iron formation of the Timeball Hill Formation in South Africa, are composed of concentric cortices of hematite (Dorland, 1999) that were likely authigenically precipitated when Fe(II)-rich waters came into contact with more oxygenated shallow seawater. Granules are either grain- or cement-supported and, in the case of the latter, it appears as though the cement precipitated early, protecting the granules from compaction and preserved "floating" textures. The presence of wave- and current-formed sedimentary structures and hummocky cross-stratification indicates that they were deposited near-shore in water depths close to or above storm and fair-weather wave base (e.g., Pufahl and Fralick, 2004).

2. What Iron Formations Tell Us About the Precambrian Environment

2.1 The major source of iron to the oceans

The abundance of iron formations in Precambrian successions was used in early studies to argue for a largely anoxic atmosphere and ocean system (e.g., Cloud, 1973; Holland, 1973, 1984). The accumulation of such large masses of iron (in the form of Superior-type BIF) required the transport of Fe(II), as Fe(III) is essentially insoluble at circumneutral pH values. Early studies invoked a continental source of iron, since Fe(II) was much more mobile during weathering in the absence of atmospheric O₂ (e.g., James, 1954; Lepp and Goldich, 1964) and potentially since continents likely had more mafic composition than today (Condie, 1993). However, detailed iron formation studies

that followed in the Hamersley Province, Western Australia, suggested that the amount of iron deposited was on the order of 1×10^{13} gm/yr (Trendall and Blockley, 1970), requiring rivers the size of the modern Amazon to transport orders of magnitude more iron than they do today. This led Holland (1973) to suggest that iron was instead sourced from deep marine waters and supplied to the depositional settings via upwelling. With the discovery of modern seafloor-hydrothermal systems (e.g., Corliss et al., 1978), the high Fe flux from slow-spreading mid-ocean ridges (Saito et al., 2013), and the recognition that modern hydrothermal systems may contribute up to 75% of dissolved iron to the Fe budget in the deep-oceans (Carazzo et al., 2013), support for a deep-sea iron source has become much stronger.

Based on rare earth element (REE) composition of iron formations, it is now generally accepted that deep-sea hydrothermal processes are the most likely source of Fe. Europium (Eu) anomalies have been central in the use of REE to trace Fe sources. Europium enrichment in chemical sedimentary rocks precipitated from seawater indicates a strong influence of high-temperature hydrothermal fluids on the seawater dissolved REE load (e.g., Klinkhammer et al., 1983; Derry and Jacobsen, 1988, 1990). The disparate behaviour of Eu from neighbouring REE in hydrothermal fluids is linked with Eu(III) reduction at high-temperature and low Eh conditions (Klinkhammer et al., 1983). It is generally assumed that Fe and REE will not be fractionated during transport from spreading ridges or other exhalative centres, and, therefore, a strong positive Eu anomaly indicates that the iron in the precursor sediment was hydrothermally derived (e.g., Slack et al., 2007). In this regard, secular trends in the magnitude of Eu anomalies in large Superior-type iron formations has historically been assumed to indicate variations in hydrothermal flux, with a long-term decrease in hydrothermal activity from the Eoarchean to Paleoproterozoic (e.g., Derry and Jacobsen, 1990; Sreenivas and Murakami, 2005). This REE trend is likely linked with an overall decline in the delivery of reductants from Earth's interior.

Isotope ratios of some REE (e.g., Ce and Nd), in addition to REE concentrations, have also been used to constrain REE and Fe sources to seawater (Tanaka et al., 1982; Derry and Jacobsen, 1990; Shimizu et al., 1991; Amakawa et al., 1996; Hayashi et al., 2004). Both Ce and Nd have short residence times in the modern ocean, 90-165 and 1000-1500 years, respectively (Amakawa et al., 1996), and the Archean oceans were likely strongly heterogeneous in their $\epsilon_{Nd}(t)$ values (which describes the deviation of the $^{143}Nd/^{144}Nd$ ratio measured in a sample relative to the $^{143}Nd/^{144}Nd$ ratio in a chondritic uniform reservoir in part per 10^4), with +1 to +2 values typical of the deep-waters dominated by hydrothermal sources and lower values, down to -3, typical of shallow-waters dominated by terrestrial sources (Miller and O’Nions, 1985; Jacobsen and Pimentel-Klose, 1988; Alexander et al., 2008). Similarly, $\epsilon_{Ce}(t)$ values in iron formations point to a strong hydrothermal influence on trace element composition of the Archean ocean (Shimizu et al., 1990; 1991).

Although it is now widely agreed that the dominant source of ferrous iron to the oceans was hydrothermal, there remains considerable uncertainty regarding the proximity of this source to the depositional settings, in particular for the Superior-type BIF. Holland (1973) was first to propose that Fe(II) was brought from the deep ocean onto the outer continental shelf by upwelling currents. In this case, the Fe source could have been distal mid-ocean-ridge systems. This then led to a depositional model suggesting that iron formations formed below wave base on partially isolated, submerged platforms on the continental shelves of older cratons, where deep ocean water was able to circulate freely, but some form of physical barrier was nonetheless required to explain the absence of terrigenous siliciclastic sediments coarser than clay size (Morris and Horowitz, 1983; Morris, 1993).

More recently, it was proposed that Fe(II) was supplied directly with hydrothermal plumes to shallow water. Archean ridge crests were likely shallower than today (Isley, 1995). Under such conditions, hydrothermal effluent could have risen buoyantly upwards through the water column to

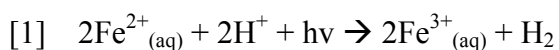
the photic zone – where a number of oxidative mechanisms could have occurred (see section below). Even in the modern oceans, hydrothermal signatures are measurable in plumes over distances of thousands of kilometres away from venting sites (e.g., Lupton, 1996), and thus Fe(II) in the Archean and Paleoproterozoic could have spread throughout much of the continental shelf where iron formations were deposited. Building upon these ideas, Isley and Abbott (1999) suggested a direct link between mantle plume activity between 3.8 and 1.8 Ga and global iron formation deposition. This view is supported by the work of Barley et al. (1997; 2005) who proposed that the ca. 2.5 Ga Hamersley BIF in Western Australia formed during a major tectono-magmatic event that caused an increased supply of dissolved Fe(II) to the oceans. While the actual quantity of dissolved Fe(II) released with hydrothermal fluids is unknown, the elevated temperatures of water-rock reactions in the Archean and the low marine sulfate concentrations (which affect the Eh of hydrothermal fluids) suggest that dissolved Fe(II) in hydrothermal effluents may have been 1 to 2 orders of magnitude higher than today (e.g., Kump and Seyfried, 2005). The concentration of Fe(II) effused from some modern deep sea vents is as high as 1.8 mM (Edmond et al., 1982). Furthermore, the observation that Archean shales are enriched in Fe, relative to average Phanerozoic shales, may also indicate a larger hydrothermal flux of Fe to the early oceans (Kump and Holland, 1992).

It is now believed that deposition of large, economically important iron formations coincided in time with mantle plume breakout events, as recorded by the secular distribution of large igneous provinces (LIPs), dike swarms, and submarine-emplaced mafic volcanic rocks (e.g., Isley and Abbott, 1999; Rasmussen et al., 2012). LIPs are linked to short-lived igneous events with magma produced in the mantle, resulting in relatively rapid intrusion and eruption of high volumes of mafic to ultramafic magma (Coffin and Eldholm, 1994; Ernst and Buchan, 2001). Higher oceanic spreading rates, increased submarine and subaerial volcanic activity, high sea-level, greenhouse

conditions, and an enhanced production of VMS deposits are predicted consequences of mantle plume breakout events (e.g., Condie et al., 2001; Barley et al., 2005).

2.2 Available oxidants in seawater for Fe(II) oxidation

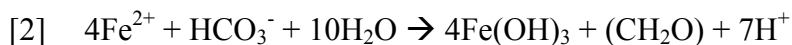
The mineralogy and Fe isotope composition of BIF dictates that some oxidation of Fe(II) was necessary for precipitation, yet which mechanism(s) dominated remains uncertain. Prior to the rise of atmospheric oxygen and the development of a protective ozone layer, the Earth's surface was subjected to high levels of ultraviolet radiation. Bulk ocean waters that were anoxic at this time could have supported high concentrations of dissolved Fe(II). Under such conditions, dissolved ferrous iron species, such as Fe^{2+} or $\text{Fe}(\text{OH})^+$, absorb radiation in the 200-400 nm range, leading to the formation of dissolved ferric iron [reaction 1], which in turn, hydrolyse to form ferric hydroxide at circumneutral pH (Cairns-Smith, 1978; Braterman et al., 1983; Anbar and Holland, 1992).



However, experiments focused on determining the specific rates of Fe(II) photochemical oxidation did not simulate the complex, disequilibrium water chemistry characteristic of an ocean where Fe(II)- and Si-rich hydrothermal waters reacted with ambient Si-saturated seawater that also contained high concentrations of HCO_3^- . Indeed, in fluids with high dissolved Fe(II), $\text{Si}(\text{OH})_4$ and HCO_3^- , the oxidation effects of either UV-C (200-280 nm wavelength) or UV-A (320-400 nm wavelength) were found to be negligible compared to the precipitation of ferrous silicates and ferrous carbonates (e.g., Konhauser et al., 2007b). The point being that although UV photo-oxidation does occur, in an ocean supersaturated with siderite and greenalite, its role may have been small.

As an alternative to the abiological model, the presence of ferric iron minerals in iron formations has also been ascribed to the metabolic activity of planktonic bacteria in the oceans' photic zone (Figure 2). Although a biological role in iron precipitation was suggested over a century ago (e.g., Leith, 1903; Gruner, 1922), the importance of bacteria began to receive greater acceptance with the discovery of microfossils in the ca. 1.9 Ga iron formations in the Animikie basin of the Lake Superior region (e.g., Tyler and Barhoorn, 1954; Barghoorn and Tyler, 1965; Cloud, 1965). Based on the assumption that the microfossils were cyanobacteria, or their predecessors, Cloud (1973) proposed that these primitive O₂-producing photosynthetic bacteria lacked suitably advanced oxygen-mediating enzymes and, consequently, required Fe(II) as an oxygen acceptor. Therefore, these microorganisms would have flourished when Fe(II) (and nutrients) were made episodically available, allowing for the indirect oxidation and precipitation of ferric oxyhydroxides, such as ferrihydrite. By contrast, the photosynthetic population declined in number when Fe(II) availability was limited. Other bacteria may have directly utilized low O₂ concentrations available in the surface waters of the Archean oceans for Fe(II) oxidation. For example, Holm (1989) speculated that oxidation of Fe(II) by chemolithoautotrophic species, such as *Gallionella ferruginea*, would have been kinetically favoured in an ocean with limited free oxygen because abiological rates of Fe(II) oxidation at circumneutral pH are slow under microaerobic conditions (e.g., Sogaard et al., 2000). Interestingly, many of the ca. 1.9 Ga Gunflint-type microfossils from the Animikie basin have been reinterpreted as chemolithoautotrophic Fe(II) oxidizers (Golubic and Lee, 1999; Planavsky et al., 2009).

A different biological model was proposed by Garrels et al. (1973) and Hartman (1984), who both suggested that light, not O₂, may have coupled the carbon and iron cycles via photosynthesis that used Fe(II) rather than H₂O as an electron donor, producing Fe(III) instead of O₂. This process is known as photoferrotrophy [reaction 2].



Since then, a number of experimental studies have confirmed that various purple and green bacteria can use Fe(II) as a reductant for CO₂ fixation (e.g., Widdel et al., 1993; Heising et al., 1999; Straub et al., 1999). The ferric iron minerals these strains produce are also consistent with the likely precursor iron formation minerals, Fe(III) precipitates (Kappler and Newman, 2004). In particular, photoferrotrophs produce amorphous to poorly crystalline ferric oxyhydroxide minerals, which carry a net positive charge. Such biogenic minerals are expected to bind to organic carbon (cells) and silica, with the net effect being the deposition of Fe-Si-C aggregates onto the sea floor (Posth et al., 2008, 2010).

2.3 Evidence in the rock record for the evolution of oxygenic photosynthesis

In order to determine the significance of different biological oxidative mechanisms that may have driven iron formation deposition it is essential to constrain when anoxygenic photosynthesis and oxygenic photosynthesis evolved. Although the timing of the evolution of cyanobacteria and photoferrotrophs are still debated, there are a number of indicators in the rock record that can be used to constrain their appearance in the Archean. In the case of cyanobacteria, this includes:

(1) Stromatolitic assemblages in the 2.7 Ga Tumbiana Formation, Western Australia, presumed to have been constructed by photoautotrophs that utilised oxygenic photosynthesis (Buick, 1992). This view is supported by the earliest recognised fossil assemblage of filamentous and coccoidal cell colonies from the ca. 2.6 Ga Campbellrand Group, South Africa, possibly including oscillatoriacean cyanobacterial genera such as *Phormidium* and *Lyngbya* (Altermann and Schopf, 1995). However,

these microbial microfossils have simple morphologies that are difficult to link to specific organisms. Further, the construction of stromatolite-like structures by the anoxygenic phototroph *Rhodopseudomonas palustris* (Bosak et al., 2007) may challenge the notion that stromatolites strictly mark cyanobacterial presence in the geologic record. It therefore seems possible that prior to the rise of cyanobacteria, predecessor anaerobes, such as anoxygenic phototrophs, were the dominant stromatolite-building organisms, accounting for the stromatolitic record predating strong evidence for oxygenic phototrophs. Lastly, and arguably, there is no stromatolitic structure that can be definitively linked to a microbial influence, even if microbially-mediated stromatolite formation seems to be the most parsimonious mode for their formation (cf., Grotzinger and Knoll, 1999).

(2) The presence of extremely isotopically depleted kerogens that have been recovered from ca. 2.72 to 2.59 Ga carbonates and shales in the Hamersley Province of Western Australia, Kaapvaal craton in South Africa, and the Superior craton in Canada. Organic-carbon $\delta^{13}\text{C}$ values in these metasediments are as low as -60‰ (Hayes, 1983; Eigenbrode and Freeman, 2006). The most ^{13}C -depleted values have been ascribed to the assimilation of methane by chemolithoautotrophic, methanotrophic bacteria that utilise electron acceptors such as O_2 , SO_4^{2-} , or NO_3^- . However, sulfate can form via photolysis of SO_2 of volcanic origin, and it might be possible to have methane oxidation via Fe^{3+} (e.g., Konhauser et al., 2005; Beal et al., 2009; Crowe et al., 2011). As outlined above, Fe(II) oxidation does not require oxygenic photosynthesis.

(3) Nitrogen isotope compositions of kerogens in minimally altered shales from the Campbellrand-Malmani carbonate platform in South Africa and broadly correlative sedimentary succession in Western Australia (Hamersley Group) show a significant rise in their $\delta^{15}\text{N}$ values between 2.67 and 2.50 Ga (Godfrey and Falkowski, 2009; Garvin et al., 2009). Exceptionally high $\delta^{15}\text{N}$ values are

also reported for the 2.72 Ga Tumbiana Formation (Thomazo et al., 2011). This positive shift has been interpreted as evidence for the onset of nitrification-denitrification reactions in the surface oceans; importantly, these microbial processes are typically thought to require the presence of oxygen. However, the emerging view is that it is possible to have anaerobic nitrification via Fe^{3+} (e.g., Yang et al., 2012; Busigny et al., 2014), making the implications of the N record more ambiguous than previously thought.

(4) Over the past decade, redox-sensitive trace element data has been generated from paleosols, shales, carbonates, and iron formations that suggests an early Archean rise of oxygenic photosynthesizers. Amongst this data, the most widely referred to are from shales in the Campbellrand-Malmani and Hamersley groups. This data includes (i) the shales with nitrogen isotope compositions suggestive of nitrification, and (ii) those that contain high concentrations of Re and Mo. Strong Re and Mo enrichments and coupled Mo-Fe isotope data were interpreted as evidence for oxidative continental sulfide weathering, and thus the evolution of oxygenic photosynthesis as early as ca. 2.6 Ga (Anbar et al., 2007; Kendall et al., 2010; Czaja et al., 2012). Further support for the appearance of oxygenic photosynthesis by 2.7 Ga comes from sulfide concentrations in marginal marine sediments (Stüeken et al., 2012). Most recently, Cr isotopes in 3.0 Ga paleosols suggest that there were appreciable levels of oxygen even at that time (Crowe et al., 2013).

(5) Bitumens from the ca. 2.6 Ga Marra Mamba Iron Formation and the ca. 2.5 Ga Mt. McRae Shale of the Hamersley Group, Western Australia yield abundant 2α -methylhopanes, derivatives of prominent lipids in cyanobacteria (methyl-bacteriohopanepolyols), which are responsible for cell membrane rigidity (Brocks et al., 1999; Summons et al., 1999). Hopanes carrying 3-methyl

substituents have also been recovered from 2.72 to 2.56 Ga carbonates and shales of the Hamersley Group (Eigenbrode et al., 2008). The only known extant bacteria to produce these particular hopanes are aerobic methanotrophs. A third suite of biomarkers, specifically steranes of 28- to 30-carbon isomers, was reported in bitumens of the ca. 2.7 Ga shales of the Roy Hill Member of the Jeerinah Formation, Fortescue Group, Western Australia (Brocks et al., 1999). These steranes are unique alteration products of the sterols used in extant eukaryotic cell membranes. Since oxygen is required for the biosynthesis of these sterols, their extraction from Archean sedimentary rock suggests that at least some dissolved oxygen (low nM [O₂]) was present at the time of their production (Waldbauer et al., 2011). Note, however, that the origin of these biomarkers remains controversial, with recent arguments favouring later contamination (see Rasmussen et al., 2008; Brocks, 2011), while others bring into question their taxonomic specificity (e.g., Rashby et al., 2007).

(6) Several weight percent concentrations of organic carbon in sedimentary rocks provide one of the most straightforward and compelling arguments for the Archean evolution of oxygenic photosynthesis. A wide range of microbial metabolisms can, of course, produce organic carbon, but only a handful of these metabolisms can realistically produce organic carbon-rich sedimentary rocks (Buick, 2008; Scott et al., 2011). Since photoferrotrophy produces a particulate iron oxide as well as organic carbon, it is more likely, as outlined above, to produce organic carbon-poor, iron-rich rocks like iron formations, because much of the organic matter would be oxidised via microbial Fe(III) reduction. Photosynthetic sulfide and H₂ oxidizers can be important primary producers and could in theory produce organic matter-rich rocks like black shales. However, the reductant for these microbial metabolisms, unlike for oxygenic photosynthesis, must be sourced from a hydrothermal system or produced via microbial degradation of organic matter. Sulfide and H₂, unlike Fe²⁺, are not

thought to have been present at significant levels in Archean water column. Therefore, it is likely that Archean organic carbon-rich sediments, distal to any sort of hydrothermal system, record the presence of oxygenic photosynthesizers. There are organic matter-rich black shales without a proximal hydrothermal influence in sedimentary successions deposited at least ca. 2.7 Ga (Buick, 2008; Scott et al., 2011).

In conclusion, although definitive evidence for oxygenic photosynthesis prior to ca. 2.5-2.4 Ga (the onset of the Great Oxidation Event, or GOE, see section 3) is lacking, it is plausible that biological oxygen production began prior to 2.7 Ga. However, given that there is evidence for oxidative processes at the depositional site of the iron formation protolith as far back as 3.8 Ga (Dauphas et al., 2008), it seems reasonable to suggest that iron formation deposition took place well before the emergence of oxygenic photosynthesis. These early deposits were likely precipitated from anoxic seawater with Fe(II) oxidation via anoxygenic photosynthesis being the most plausible mechanism for Fe(III) precipitation.

2.4 Evidence in the rock record for the evolution of photoferrotrophy

There is even less actual physical and chemical evidence for the existence of Fe(II)-oxidising phototrophs in the Archean. However, their presence can be inferred from the following:

(1) Of the seven strains of anoxygenic Fe(II)-oxidising phototrophs known to date, six have been classified as *Proteobacteria* and one as a green sulfur bacterium (Posth et al., 2012). This large and diverse phyla of bacteria likely diversified from an ancestral anoxygenic phototroph (Woese, 1987); molecular phylogenetic analysis of a number of enzymes involved in (bacterio)-chlorophyll biosynthesis suggests that anoxygenic photosynthetic lineages are likely more deeply rooted than the oxygenic cyanobacterial lineages (Xiong, 2006).

(2) Anoxygenic phototrophs are able to utilize multiple substrates (e.g., H_2 , H_2S , Fe^{2+}), but throughout the Archean, ferrous iron was likely the main reductant in seawater until its supply became diminished with deep-water oxygenation; only with its depletion did the marine biosphere evolve alternate electron donors (potentially with an H_2O_2 or Mn intermediate) in the cyanobacterial line of evolution (Olson and Blankenship, 2004; Allen et al., 2012). There is evidence for euxinic (anoxic and sulfidic) conditions as far back as 2.64 Ga (Scott et al., 2011), but the spatial extent of those euxinic waters was likely limited.

(3) Based on REE data it appears that there was no discrete redoxcline in the depositional basins of multiple Archean iron formations (Planavsky et al., 2010a). However, multiple sedimentological and geochemical lines of evidence point to low Fe(II) in shallow waters (e.g., Sumner, 1997). The simplest explanation for these two sets of observations is the presence of anoxygenic Fe(II) oxidation (and by default photoferrotrophs) at depth which consumed the upwelling Fe(II) before it reached shallow waters. This water column structure contrasts strongly with that during deposition of iron formations after the rise of atmospheric oxygen, where Fe(II) oxidation took place by a combination of microbial oxidation below the chemocline and abiotic, oxygen-mediated Fe(III) precipitation at the redoxcline (e.g., Planavsky et al., 2010a).

(4) Numerical models have been used to suggest that anoxygenic photosynthesizers would control Fe(II) oxidation even if the surface layer was oxygenated (Kappler et al., 2005). This model is based on the simple idea that a layer of photoferrotrophs could thrive beneath an oxygenated surface layer even at low levels of photosynthetically active light. The model employs Fe(II) oxidation rates from modern anoxygenic photosynthesizers under a range of reasonable mixing rates in the ocean. This

directly contrasts with the recent suggestion by Czaja et al. (2012), based on a simple dispersion-reaction model, in which extensive water column Fe(II) oxidation requires significant levels of dissolved oxygen. The latter model infers that abundant iron formation deposition in the Late Archean was not linked to anoxygenic photosynthetic Fe(II) oxidation.

In the case of point (4), the strong contrast between these two modelling efforts invites a detailed analysis of the assumptions and parameter choices in each model. At the heart of this contrast, Czaja et al. (2012) suggested that because Fe(III) deposition was focused in the deep basins, and not in shallow-water environments, anoxygenic photosynthesizers could be ignored. This argument, however, can be questioned given that iron is likely to be sourced from deep-water hydrothermal systems (rather than continents) in most Archean basins, opening up the possibility that the depth of the iron chemocline could be biologically controlled. In fact, the Kappler et al. (2005) model was meant to directly test the idea of a biotic (internal marine) regulation on the depth of the iron chemocline. The latter model provides a mechanism for precipitation of Fe(III) compounds without surface water oxygenation.

Kappler et al. (2005) presented a model for determining the thickness of a layer with photoferrotrophic bacteria required to fully oxidize a hydrothermal source of Fe(II) at a variety of Fe(II)-oxidation rates in a marine system. The model considers eddy-diffusion as the dominant mode of transport for Fe(II), essentially assuming that diapycnal diffusivity was the main transport term. At a conservative, experimentally-based, depth-integrated phototrophic Fe(II)-oxidation rate of 1.4×10^{-5} M/day (corresponding to a depth of 100 m), an estimated Fe(II) concentration of 0.5 mM, and the modern global mean eddy-diffusion rate of $0.1 \text{ cm}^2/\text{s}$, it was estimated that a photoferrotrophic bacterial layer of 17.6 m thick was required to completely oxidize the Fe(II)

input. This result suggests that such bacteria could potentially have oxidised all of the upwelling Fe(II) in the Precambrian oceans.

One potential problem with this approach is that in many settings advection can be the dominant transport process (e.g., upwelling zones). As a simple test to assess the required thickness of a photoferrotrophic bacterial layer to oxidize both upwelling and diffusive Fe(II) inputs, we add upwelling as a mode of Fe(II) transport to the Kappler et al. (2005) model. The thickness required to quantitatively oxidise upwelling iron is calculated similarly to Kappler et al. (2005) using the expression: $z = \omega \times \Delta C / (d\text{Fe(II)}/dt)$, where ω represents advection or upwelling rate, ΔC is the iron concentration gradient from the bottom to the top of the Fe(II)-oxidising bacterial community, and $d\text{Fe(II)}/dt$ is the rate of photoferrotrophic Fe(II)-oxidation. The calculated thickness is then added with that for eddy-diffusion, using the modern global mean eddy diffusivity of 0.1 cm²/sec. Results with a ΔC of 0.5 mM and 0.1 mM and upwelling rates of 0.5 m/day and 5 m/day are shown in Figure 3. Modelled advection rates (0.5 and 5 m/day) fall within the average and high of the range of annual averages observed in continental upwelling zones (e.g., Canfield, 2006).

Not surprisingly the thickness of the photosynthetic Fe(II)-oxidising bacterial layer increases when advection is considered as opposed to solely eddy-diffusion transport. The thickness of the photoferrotrophic bacterial layer is quite sensitive to upwelling rates, especially at low rates of Fe(II) oxidation. At the conservatively estimated Fe(II)-oxidation rate of 1.4×10^{-5} M/day and an Fe(II) concentration of 0.1 mM, a 34 m or >100 m thick layer of Fe(II)-oxidising bacteria is required to fully oxidize the Fe(II) input at upwelling rates of 0.5 and 5 m/day, respectively (Figure 3). These estimates are significantly larger than the 17.6 m thickness calculated with eddy-diffusion alone. Furthermore, this result indicates, considering the expected range of upwelling conditions and reasonable rates of photoferrotrophic Fe(II) oxidation, a wide scope in the extent of Fe(II) oxidation in Archean water masses. In fact, given that upwelling is highly variable on a seasonal

time scale (with shifts over an order of magnitude in some settings), a variable extent of oxidation is likely to characterise any Archean setting where upwelling was an important transport vector. However, this does not mean that a layer of photoferrotrophic bacteria could not quantitatively oxidise upwelling iron in a wide range of environments, in contrast to the recent suggestion by Czaja et al. (2012).

Consistent with the idea of partial oxidation prevailing in the water column, highly variable, but generally negative Fe isotope values in sedimentary pyrite from the ca. 2.9-2.3 Ga black shales (0.5‰ to -3.5‰) likely reflect the initial deposition of ferric oxyhydroxides (e.g., as a mineral precursor for iron formation), which preferentially removed isotopically heavy Fe, driving the ocean waters to the negative $\delta^{56}\text{Fe}$ compositions (Rouxel et al., 2005). The iron isotope record is therefore fully consistent with enzymatic oxidation of the dissolved Fe(II) that was brought into the surface waters by eddy-diffusion and upwelling.

2.5 Available reductants and diagenesis of iron formations

If a biological mechanism was important in Fe(II) oxidation in the ancient ocean water column, it could be expected that biomass would have settled to the seafloor along with the Fe(III) minerals (e.g., Konhauser et al., 2005; Li et al., 2011; Posth et al., 2013a,b). Given that the bulk water column was anoxic, perhaps with the exception of local oxygen oasis (e.g., Kasting, 1992), the ferric minerals would have represented a favourable electron acceptor for the oxidation of organic matter (Walker, 1984; Nealson and Myers, 1990) through dissimilatory iron reduction (DIR) by bacteria. Significantly, coupling the reduction of Fe(III) minerals to the oxidation of organic matter not only explains the low content of organic carbon in iron formations (<0.5 wt%; Gole and Klein, 1981), but it also explains negative carbon isotope values associated with the early diagenetic carbonates (Perry et al., 1973; Walker, 1984; Baur et al., 1985) and the general lack of microfossils

preserved in the Fe-rich layers. Moreover, these post-depositional processes would have modified the initial precursor sediment into the mineral assemblages observed today (Figure 4).

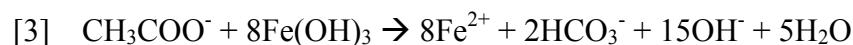
Supporting evidence for an ancient Fe(III) reduction pathway comes from the observation that many deeply-branching *Archaea* (i.e., some of the oldest purported species) are capable of using H₂ to reduce Fe(III) to support chemolithoautotrophic growth (Vargas et al., 1998). They can even use quinone moieties as electron shuttles between solid-phase iron minerals and H₂, thereby alleviating the need for direct contact between the cell and mineral surface (Lovley et al., 2000). Moreover, Fe(III) reduction has been shown to be broadly distributed amongst several known *Proteobacteria* genera, suggesting that this form of metabolism became widespread over the course of evolution (Barns and Nierzwicki-Bauer, 1997).

There is also tentative mineralogical and isotopic evidence of ancient microbial Fe(III) reduction in Precambrian sedimentary rocks. For instance, the spheroidal forms of siderite found in several iron formations are similar to the siderite grains formed experimentally when ferrihydrite reacted with organic carbon at pressure and temperature conditions commensurate with iron formation diagenesis (Köhler et al., 2013). Likewise, the large magnetite grains found in iron formations can be replicated experimentally through a three-stage sequence, beginning with DIR of an initial ferric iron-rich sediment coupled to the oxidation of dead phytoplankton biomass, followed by magnetite crystal aging, and ultimately pressure-temperature induced abiotic alteration of the biogenic magnetite during metamorphism (Li et al., 2013). Moreover, siderite as far back as 3.8 Ga contains positive $\delta^{56}\text{Fe}$ values that must be linked to a sedimentary flux of ferric oxyhydroxides to the sediment-water interface (Dauphas et al., 2007). Iron isotope systematics, therefore, necessitates that there was an initial ferric iron flux to the sediment pile and that this ferric iron must have been reduced and re-precipitated as siderite. A plausible pathway for this reaction is DIR (e.g., Johnson et al., 2008; however, see also Planavsky et al., 2012a for evidence in

support of a metamorphic origin). Light iron isotope values have also been linked to DIR and the benthic shuttling of iron from reducing shelf sediments to anoxic deep basins (e.g., Severmann et al., 2008); while, as mentioned above, heavier Fe isotope signatures can also be explained by partial Fe(II) oxidation (Rouxel et al., 2005). Importantly, these two models are not mutually exclusive. For instance, it has been proposed recently that while the bulk chemistry of iron formations reflect seawater composition, small-scale heterogeneity may reflect subsequent fractionation during diagenesis and metamorphism (e.g., Frost et al., 2007; Steinhofel et al., 2010; Planavsky et al., 2012a).

Quantifying the significance of microbial Fe(III) reduction in the Precambrian is, however, extremely difficult, considering the post-depositional alteration of the rocks and the lack of modern analogues. Furthermore, although estimates can be made regarding the quantity of reducing equivalents necessary to account for the diagenetic Fe(II) component in Fe-rich layers, those estimates do not offer any insights into the magnitude of Fe(III) generated within the water column and, hence, the efficiency of Fe and C recycling prior to burial. In an attempt to address these uncertainties, Konhauser et al. (2005) modelled the ancient Fe cycle based simply on conservative experimental rates of photosynthetic Fe(II) oxidation in the photic zone. They showed that under ideal growth conditions, as much as 70% of the biologically produced Fe(III) could have been recycled back into the water column via fermentation and organic carbon oxidation coupled to microbial Fe(III) reduction. By comparing the potential size of biomass generated phototrophically with the reducing equivalents required for Fe(III) reduction and magnetite formation, they also hypothesised that another anaerobic metabolic pathway might have been utilised in the surface sediment to oxidise organic carbon. Based on the premise that the deep ocean waters were anoxic, this role could have been fulfilled by a consortium of fermenters and methanogens (Konhauser et al., 2005; Figure 2).

We can gain a better mechanistic understanding of the pathways of organic matter remineralisation and explore the possibility of methane cycling in precursor sediments to iron formations with a simple diagenetic modelling of DIC pore-water profiles and the current iron formation carbonate-carbon isotope record (Figure 5). Archean iron formations have $\delta^{13}\text{C}$ values as low as -16‰, typically found in Fe-rich carbonates (Fischer et al., 2009). These low carbon isotope values have traditionally been explained (e.g., Walker, 1984) as resulting from the mixing of dissolved inorganic carbon (DIC) from seawater and remineralization of organic carbon during DIR [reaction 3], as opposed to further carbon inputs from Fe(III)-induced methane oxidation [reaction 4].



However, the latter possibility has yet to be tested with simple numerical models that take into account the depositional setting of iron formations and realistic Archean seawater chemistry. Previous studies have made mechanistic predictions for iron formation carbonate carbon isotope values based on stoichiometric arguments (e.g., Heimann et al., 2010). In an effort to test the potential for the observed carbon isotope values to result solely from the mixing of DIC from seawater and organic carbon remineralisation, we use a basic mass balance model to explore a range of environmental conditions. For simplicity, the accompanying buffering effects and carbonate precipitation/dissolution linked with a dynamic DIC reservoir were ignored. The $[\text{DIC}]_{\text{total}}$ was calculated using a modified version of the general diagenetic equation presented in Berner (1964); see equation A below. The three terms of this equation describe the processes of ionic diffusion, deposition and compaction, and the input of DIC into the pore-waters from organic matter

remineralisation, respectively. In this equation, G_0 is the concentration of organic carbon at the sediment/water interface; D and ω are the diffusion coefficient in the whole sediment and the sum of deposition and compaction, respectively; k is the rate of organic carbon re-mineralisation (calculated from ω ; Boudreau, 1996); z is depth in the sediment; C is [DIC]; t is time; and L is a stoichiometric coefficient describing the ratio between the amount of Fe(III) moles reduced for every carbon mole oxidised. The model is tuned to have organic mineralisation generally describing anoxic remineralization (Boudreau, 1996).

$$[A] \quad \frac{\partial C}{\partial t} = D \frac{\partial^2 C}{\partial z^2} - \omega \frac{\partial C}{\partial z} + kLG_0 \exp\left[-\frac{k}{\omega}z\right]$$

The general solution for this expression was obtained assuming steady state, $\frac{\partial C}{\partial t} = 0$, and the boundary condition $C = C_\infty$, giving the following analytical solution [equation B]:

$$[B] \quad C(z) = -\frac{\omega^2 LG_0}{Dk + \omega^2} \exp\left[-\frac{k}{\omega}z\right] + C_\infty$$

A basic assumption of the model is that a constant DIC concentration, C_0 , is contributed from seawater to the sediment profile and is equal to the DIC concentration of the overlying water column. Such an assumption allows for the use of the boundary condition, $C_0 = [\text{DIC}]_{\text{sw}}$, with equation C providing solution for C_∞ . Substituting equation C into equation B, the final solution for $[\text{DIC}]_{\text{total}}$ is obtained [equation D].

$$[C] \quad C_\infty = \frac{\omega^2 LG_0}{Dk + \omega^2} + C_0$$

$$[D] \quad C(z) = -\frac{\omega^2 LG_0}{Dk + \omega^2} \exp\left[-\frac{k}{\omega} z\right] + \frac{\omega^2 LG_0}{Dk + \omega^2} + C_0$$

Simply taking the difference between $[DIC]_{\text{total}}$ and $[DIC]_{\text{SW}}$ to determine $[DIC]_{\text{OM}}$, the mass balance relationship can be implemented to determine the carbon isotope composition of the DIC pore-water reservoir [equation E]. The model accounts for isotopic inputs of DIC from seawater ($\delta^{13}\text{C}_{\text{SW}} = 0\text{‰}$) and the remineralisation of organic matter during microbial Fe(III)-reduction ($\delta^{13}\text{C}_{\text{OM}} = -25\text{‰}$), with the isotopic values held constant and only the fluxes of DIC from each source varied with depth. This basic approach is widely used to model modern marine carbon isotope profiles, despite the intrinsic model simplifications:

$$[E] \quad [DIC]_{\text{Total}} \delta^{13}\text{C}_{\text{Total}} = [DIC]_{\text{OM}} \delta^{13}\text{C}_{\text{OM}} + [DIC]_{\text{SW}} \delta^{13}\text{C}_{\text{SW}}$$

With this approach it is straightforward to illustrate the main processes that will control the pore-water DIC carbon isotope values. Importantly, decreasing the sedimentation rate and initial utilisable organic carbon concentrations, and increasing the size of the marine DIC reservoir will result in heavier $\delta^{13}\text{C}_{\text{DIC}}$ values. This is relevant for Archean iron formations since there is almost unanimous agreement that (i) the size of the DIC reservoir was significantly larger in the Archean than in the modern ocean, (ii) most iron formation precursor sediments were deposited in offshore environments with limited siliciclastic input and low sedimentation rates, and (iii) there was proportionally more Fe(III) than organic carbon buried with iron formation precursor sediments relative to typical modern continental margin sediments.

The effects of sedimentation rate, concentration of initial reactive organic carbon, and size of the marine DIC reservoir on pore-water profiles are illustrated here by comparing conditions likely to be characteristic of iron formation precursor sediments with those typical of modern continental

margin sediments. In this case, we use a site in the Santa Barbara basin as representative of the continental margin sediment column. This site is noteworthy for its role in the development of early diagenetic modelling (Berner, 1964), but it is also fairly representative of modern marginal settings with high organic carbon loading and high rates of sulfate reduction. With the modern DIC reservoir, along with sedimentation rates and organic carbon loads characteristic of continental margin settings, $\delta^{13}\text{C}$ values of pore-water DIC quickly (within upper 20 cm) becomes highly depleted ($\delta^{13}\text{C}_{\text{DIC}} < -20\text{‰}$). However, with sedimentation rates and initial metabolisable organic carbon concentrations an order of magnitude less than those typical of continental margin sediments, and a DIC reservoir an order of magnitude larger than the modern one, the pore-water DIC $\delta^{13}\text{C}$ values would stabilise at values heavier than -6‰ (Figure 5). This magnitude of offset relative to modern marginal sediments seems likely for iron formation precursor sediments. In addition, although iron formation sedimentation was likely highly pulsed and variable (Bekker et al., 2010), it is likely that they were characterised by slow net accumulation rates linked to the low siliciclastic flux that allowed for accumulation of pure chemical sediments. Metabolisable organic carbon concentrations in precursor sediments were likely very low. For instance, iron-rich sediments populated by Fe(II)-oxidising bacteria near a hydrothermal system within the suboxic zone at Loihi seamount, which can serve as an analogue for iron formation precursor sediments (Edwards et al., 2011), are characterised by undetectable growth rates in the absence of organic carbon augmentation (Emerson, 2009). Lastly, as mentioned above, it is generally accepted that the DIC reservoir was much larger in the Archean; in this context, an estimated ten-fold greater size compared to that of the modern reservoir seems reasonable (Ridgwell and Zeebe, 2005). Consequently, the iron formation carbonate carbon isotope record is entirely consistent with significant levels of anaerobic carbon cycling in the precursor sediments. In fact, the large spread in iron formation carbonate carbon isotope values and markedly light values are exactly what would

be expected in the presence of Fe(III)-mediated organic carbon and methane oxidation in the upper part of the sediment pile.

2.6 Iron formations as tracers of seawater redox

Iron formations are among the most widely used lithologies to investigate the composition of the ancient oceans because their precursor minerals, such as ferric oxyhydroxides, are likely to retain the chemical signature of seawater (e.g., Bau and Dulski, 1996; Jacobsen and Pimental-Klose, 1988; Bjerrum and Canfield, 2002; Bolhar et al., 2004). Moreover, many iron formations contain low concentrations of crustally-sourced elements, such as Al, Ti, Zr, Th, Hf, and Sc, which implies an authigenic origin.

In addition to constraining the secular trend in the magnitude of Eu anomaly in Superior-type iron formation (discussed above), REE studies have focused on water column redox REE behaviour. These studies have drawn from a sound understanding of REE cycling in modern anoxic basins (Figure 6A). In general, oxygenated marine settings display a strong negative Ce anomaly when normalised to shale composite ($Ce_{(SN)}$), while suboxic and anoxic waters lack significant negative $Ce_{(SN)}$ anomalies and can even show positive anomalies (e.g., German and Elderfield, 1990; Byrne and Sholkovitz, 1996). Oxidation of Ce(III) to Ce(IV) greatly reduces Ce solubility, resulting in its preferential removal onto Mn(IV)-Fe(III)-oxyhydroxides, organic matter, and clay particles (Byrne and Sholkovitz, 1996). In contrast, suboxic and anoxic waters lack significant negative $Ce_{(SN)}$ anomalies due to reductive dissolution of settling Mn(IV)-Fe(III)-oxyhydroxide particles (German et al., 1991; Byrne and Sholkovitz, 1996). Similarly, light REE depletion develops in oxygenated waters due to preferential removal of light versus heavy REE onto Mn(IV)-Fe(III)-oxyhydroxides and other particle-reactive surfaces. As a result, the ratio of light to heavy

REEs markedly increases across redox boundaries due to reductive dissolution of Mn(IV)-Fe(III)-oxyhydroxides (German et al., 1991; Byrne and Sholkovitz, 1996).

In many Archean and early Paleoproterozoic iron formations there are no Ce anomalies, and thus no deviation from trivalent Ce behaviour (e.g., Fryer, 1976; Bau and Moller, 1993; Bau and Dulski, 1996; Bau et al., 1997; Alexander et al., 2008; Frei et al., 2008), suggesting that the water column from which ferric oxyhydroxides precipitated was anoxic (Bau and Dulski, 1996). In support of this model, a recent survey of 18 different Paleoproterozoic and Archean iron formations did not display significant Ce anomalies until after atmospheric oxygenation at ca. 2.5-2.4 Ga (Planavsky et al., 2010a). There are several reported cases of Ce anomalies in Archean iron formation (e.g., Kato et al., 2006). However, in some of these cases the anomalies can be linked to analytical artefacts or analysis of samples that have experienced supergene alteration (for details see Braun et al., 1990; Valetton et al., 1997; Planavsky et al., 2010a; Bekker et al., 2010). Additional work is needed to verify the existence of extensive Ce oxidation in the Archean. Additionally, it is important to note that Ce anomalies need not develop only within the water column of a basin. For instance, Ce anomalies can develop in groundwater systems (Johanneson et al., 2006).

There also appear to be differences in trivalent REE behaviour in iron formation before and after the permanent rise of atmospheric oxygen. Late Paleoproterozoic iron formation show significant ranges in light-to-heavy REE ($\text{Pr}/\text{Yb}_{(\text{SN})}$) ratios, both below and above the shale composite value (Planavsky et al., 2010a). This range of light-to-heavy REE and Y/Ho ratios in late Paleoproterozoic iron formation likely reflects variable fractionation of REE + Y by Mn(IV)-Fe(III)-oxyhydroxide precipitation and dissolution. This interpretation implies deposition of late Paleoproterozoic iron formation at ca. 1.89 Ga in basins with varying redox conditions and a strong redoxcline separating an upper oxic water column from deeper waters that were suboxic to anoxic (Planavsky et al., 2009; Figure 6B). These ranges are also similar to those seen in modern anoxic

basins. In contrast, most Archean and early Paleoproterozoic iron formation deposited before the rise of atmospheric oxygen are characterised by consistent light REE depletion (Planavsky et al., 2010a; Figure 6C). This consistent depletion in light REE suggests the lack of a discrete redoxcline and points toward O₂-independent Fe(II) oxidation mechanisms.

3. Neoarchean-Paleoproterozoic Iron Formations

The Neoproterozoic to middle Palaeoproterozoic (~2.8-1.9 Ga) marks one of the most important periods in Earth's history, with a number of major interlinked environmental and biological evolutionary events. These include, amongst others, the evolution of oxygenic photosynthesis and the development of an oxic layer in the oceans (see previous discussion) and ultimately the oxygenation of the atmosphere – the GOE (Bekker et al., 2004, Konhauser et al., 2011). The GOE represents a transition from the atmosphere that was essentially devoid of free oxygen (O₂ << 10⁻⁵ present atmospheric levels, PAL) to one with O₂ concentrations >10⁻⁵ PAL (Pavlov and Kasting, 2002). In the rock record this event is manifested by a number of changes (see Farquhar et al., 2011, for review), including (1) loss of easily oxidisable detrital uraninite, pyrite, and siderite in fluvial siliciclastic sediments around 2.4 Ga (e.g., Rasmussen and Buick, 1999; England et al., 2002; Hofmann et al., 2009); (2) loss of iron in ancient soil horizons (paleosols) older than around 2.4 Ga because of the greater solubility under reducing conditions (e.g., Rye and Holland, 1998); (3) the appearance of red beds after ca. 2.3 Ga (e.g., Roscoe, 1969; Chandler, 1980; Melezhik et al., 2005); (4) the presence of significant mass-independent fractionation of sulfur isotopes (S-MIF) in sulfide and sulfate minerals in sedimentary rocks deposited prior to 2.4 Ga, but not after 2.3 Ga (Farquhar et al., 2000; Bekker et al., 2004; Papineau et al., 2007; Partridge et al., 2008; Guo et al., 2009; Williford et al., 2011); and the increase in Cr and U contents in BIF at 2.45 Ga that records the onset of oxidative continental weathering (Konhauser et al., 2011; Partin et al., 2014).

3.1 Iron formations deposited before the GOE

Iron Formations deposited between 2.60 and 2.45 Ga are the most laterally extensive and economically valuable of any time in Earth's history. The ca. 2.60 Ga Marra Mamba Formation of the Hamersley Province in Western Australia is one of the thickest sediment-hosted BIF in the geologic record. It was deposited in a deep-water basinal setting adjacent to a passive margin during the sea-level highstand of the Marra Mamba Supersequence and has an average thickness of about 210 m (Trendall and Blockley, 1970; Krapež et al., 2003). The BIF carries a pronounced positive Eu anomaly (Alibert and McCulloch, 1993), suggesting a strong hydrothermal imprint on REE systematics of the global ocean during its deposition.

Only one, yet economically-insignificant, iron formation (Bruno's Band) occurs in the Hamersley Province stratigraphically between the ca. 2.60 Ga Marra Mamba Formation and the overlying 2.50-2.45 Ga iron formations (Krapež et al., 2003); none occur between 2.60 and 2.50 Ga in the Transvaal Province in South Africa (Beukes and Gutzmer, 2008). This younger episode in iron deposition corresponds closely with volcanism during a 2.50-2.45 Ga series of mantle plume breakout events of global extent (e.g., Heaman, 1997) and is immediately preceded by the final stage in the supercontinent assembly well-dated on the Gawler craton (Southern Australia), North China craton, East Antarctica, and in the Central Indian Tectonic Zone of India (Barley et al., 2005). Deposition of these iron formations occurred on a reactivated continental margin (Krapež et al., 2003) during a rise in sea level. In addition to these Australian deposits, those in the Quadrilátero Ferrífero region in Brazil, Middleback Ridge (Gawler craton) in South Australia, Krivoy Rog area in Ukraine, and Kursk Magnetic Anomaly (KMA) region in Russia are broadly similar in age based on available geochronological and chemostratigraphical constraints, as well as on similar pattern of macrobanding (Prilutzky et al., 1992; Kulik and Korzhnev, 1997; Bekker et al., 2003; Spier et al.,

2007; Szpunar et al., 2011). These iron formations were also deposited on reactivated continental margins and are separated by a prominent unconformity from overlying Paleoproterozoic sequences. The unconformities correspond to a long gap in sedimentation following the supercontinent assembly at ca. 2.40 Ga. Assuming that these iron formation are similar in age, more than 60% of the known iron resources were deposited during the time interval 2.60-2.40 Ga (Isley and Abbott, 1999).

3.2 Minor iron formation deposition after the GOE and before ca. 1.88 Ga

Giant iron formations were not deposited between ca. 2.40 and 1.88 Ga. Nonetheless, sediment-hosted and volcanic-hosted deposits are known from this time period. Shortly after the rise of atmospheric oxygen at ca. 2.40 Ga, oolitic hematitic ironstones of the lower Timeball Hill Formation in South Africa were deposited in shallow-water, above fair-weather wave base (Schweigart, 1965; Dorland, 1999). Few geochemical data are available for this unit, partly because it contains significant amounts of siliciclastic material. Its deposition at ca. 2.32 Ga (Hannah et al., 2004) may coincide with a magmatic event at that time (e.g., Eriksson et al., 1994a, b; Fetter et al., 2000; Berman et al., 2005; Hartlaub et al., 2007). However, the significance of this magmatic event is poorly known. Correlative iron formations are not documented on other continents.

The Hotazel Formation in South Africa is commonly thought to have been deposited around 2.22 Ga. However, the depositional age has also been estimated to be around 2.40 Ga based on a carbonate Pb-Pb age (Bau, 1999). The Hotazel Formation contains BIF interlayered with manganese-rich sedimentary rocks; this is the largest known manganese deposit in the world (Tsikos et al., 2003). The iron and manganese formation lies above, and may be genetically related to, the submarine-emplaced Ongeluk Lavas. The iron- and manganese-rich interval of the Hotazel Formation consists of three upward-shallowing sequences deposited in a continental shelf

environment (Schneiderhan et al., 2006). Significantly, the deposits lack positive Eu anomalies but have pronounced negative Ce anomalies, suggesting an oxygenated state for the coeval deep ocean (Tsikos and Moore, 1997). Absence of a significant Eu anomaly is also important because it indicates that the global ocean was not dominated by a hydrothermal high-temperature flux at that time and that Fe and Mn were probably derived locally, within the basin, by relatively shallow-water alteration of the underlying thick (~1 km) sequence of volcanic rocks. If the Hotazel Formation was deposited at 2.22 Ga, it coincides with the largest positive carbon isotope excursion in Earth's history, the Lomagundi Event, which appears to be related to high relative burial rates of organic carbon and associated oxygen release to the atmosphere (e.g., Schidlowski et al., 1976; Karhu and Holland, 1996; Bekker et al., 2001). This REE pattern may, therefore, indicate that significant parts of the oceans were already oxygenated by that time and that Fe(II) and Mn(II) were soluble only in isolated to semi-isolated basins overwhelmed by a hydrothermal flux of reduced solutes.

Hematitic oolites and hematite-rich sandstones continued to be deposited in shallow-marine environments during the ca. 2.25 to 2.10 Ga Lomagundi carbon isotope excursion in South Africa (e.g., Silverton Formation; Schweigart, 1965) and on the Kola Peninsula in Russia (Kuetsjärvi Sedimentary Formation; Akhmedov, 1972a). The BIF deposited during the Lomagundi excursion include those within the Ijil Group, Mauritania (Bronner and Chauvel, 1979) and the Lomagundi Group, Zimbabwe (Master, 1991). The former belongs to the 2.20-2.10 Ga Birimian basin in West Africa, which also contains iron and manganese formations in the Francevillian basin, Gabon (Leclerc and Weber, 1980) and in the Nigerian schist belts (Mücke, 2005). The latter developed within the ca. 2.2-2.1 Ga Magondi belt (Master, 1991; Master et al., 2010). Volcanic-hosted iron formations deposited during the Lomagundi carbon isotope excursion are known in Brazil (e.g., Aimbè Formation, Guarinos Group; Resende and Jost, 1995; and Itapicuru Complex of the Rio

Itapicuru greenstone belt; Dalton de Souza et al., 2003) and Norway (Iddjajav'ri Group, Karasjok greenstone belt; Often, 1985).

Iron formations deposited between 2.40 and 2.10 Ga are distinctly different in scale and in most cases depositional setting compared to those of the Archean. It seems that either the deep-ocean redox state was too oxidised, relative to the strength of hydrothermal input, to form giant sedimentary iron deposits during this time interval or that marine sulfate levels were high enough that the sulfide produced during bacterial sulfate reduction exceeded the hydrothermal Fe(II) supply – in this case iron sulfides would precipitate instead of iron oxides (see Kump and Seyfried, 2005 for more discussion). Several independent lines of evidence point toward high (mM) sulfate levels during the Lomagundi Event (Schroeder et al., 2008; Planavsky et al., 2012b), consistent with the idea that growth of the marine sulfate reservoir challenged the hydrothermal iron flux, which ultimately exerted a first-order control on the distribution and abundance of iron formation.

Following the end of the Lomagundi carbon isotope excursion at ca. 2.10 Ga, small, volcanic-hosted iron formation were deposited in several basins in North America (e.g., Homestake Iron Formation, Black Hills, South Dakota; Frei et al., 2008) and Finland (Paakola, 1971; Laajoki and Saikkonen, 1977). Oolitic hematitic ironstone is also present in the Kolasjoki Formation, Kola Peninsula, Russia (Akhmedov, 1972b). Combined, these data tentatively suggest that dynamic ocean redox conditions were established in the aftermath of the GOE, with periodic upwelling of iron into shallow-water settings above storm and fair-weather wave base. However, it is also possible that these small, locally-developed iron formations are linked to a local, continental iron source (e.g., Fe-rich groundwater) rather than upwelling of ferruginous waters. This alternative has not been tested so far and requires further consideration.

An exciting, and perhaps unexpected, finding to come out of some recent studies on temporal trends in IF (and black shale) trace metal content is that the Earth's redox fabric may have been

much more complicated than previously thought. Partin et al. (2013, 2014) recently showed that directly following a dramatic increase in the oceanic uranium reservoir during the GOE, the U reservoir decreased significantly after 2.10 Ga, resulting in an U content in IF and shales that was only marginally higher than pre-GOE levels. Given that the oxygen content of the atmosphere directly controls U supply via oxidative weathering, the decrease could be due to a subsequent drop in the level of atmospheric oxygen following the Lomagundi event. It certainly seems plausible that the net organic carbon burial associated with oxygen production during the Lomagundi event later became an oxygen sink as the organic matter became oxidised, driving oxygen to low levels that may have persisted for some hundreds of million years thereafter (Bekker and Holland, 2012; Canfield et al., 2013).

3.3 The ca. 1.88 Ga resurgence in iron formations

Extensive and large iron formations reappear after an approximately 500 million year gap, at about 1.88 Ga. These successions contain an abundance of GIF, relative to Archean and early Paleoproterozoic BIF. The most extensive 1.88 Ga GIF occur in North America along the southern, and eastern margins of the Superior craton (Animikie and Mistassini basins and Labrador Trough; Simonson, 2003) and in Western Australia (Nabberu basin; Rasmussen et al., 2012). These GIF are coeval with emplacement of a ca. 1.88 Ga ultramafic to mafic LIP (Heaman et al., 1986, 2009; Hulbert et al., 2005) that is potentially related to a mantle plume breakout event during the early stage in assembly of Laurentia (Hamilton et al., 2009; for an opposing view, see Heaman et al., 2009). Recognised now to be correlative based on high-precision geochronology (Findlay et al., 1995; Machado et al., 1997; Fralick et al., 2002; Schneider et al., 2002; Stott et al., 2010), the North American GIF extend discontinuously at the surface for more than 3000 km along the southern and eastern margins of the Superior craton, from Thunder Bay, Ontario, through Minnesota, Wisconsin,

and Michigan, to Quebec (Mistassini basin) and the Labrador Trough. Correlative and texturally similar GIF are also recognised in the northern part of the Superior craton in the Hudson Bay region (Richmond Bay and Belchers islands) and in the Sutton Inliers, and are considered to have been deposited in extensional basins with coeval submarine basaltic volcanism (Fralick et al., 2002; Schulz and Cannon, 2007; Ricketts et al., 1982). These workers have proposed a back-arc setting, whereas others have advocated a foreland basin setting (Hoffman, 1987; Ojakangas et al., 2001; Schneider et al., 2002).

An intriguing question is whether deposition of these GIF represents local, basin-scale conditions or the composition and redox state of the global ocean. This is a critical issue because the occurrence and ages of these rocks have been used by some workers to infer deep-water anoxic conditions in the coeval global ocean (e.g., Poulton et al., 2004; Slack and Cannon, 2009); however, if deposition of these GIF reflects restricted, basin-scale conditions, our understanding of the ocean redox state might be incorrect. Present palaeogeographic reconstructions are insufficient to answer this question; however, tidal signatures have been observed in GIF and interbedded sedimentary rocks in Minnesota and the Hudson Bay region (Ojakangas, 1983; Chandler, 1984), which is consistent with at least periodically open-marine conditions during iron formation deposition, albeit very shallow. Two independent approaches can be used to address this issue. First, do sedimentary successions of similar age on the margins of other cratons provide evidence for high concentrations of iron in seawater? Second, do iron-oxide exhalites exist in coeval, deep-water, VMS deposits?

The ca. 1.88 Ga Frere Iron Formation, deposited along the northern margin of the Yilgarn craton of Western Australia (Goode et al., 1983; Rasmussen et al., 2012), and GIF of the Gibraltar Formation in the Kahochella Group, which developed along the southeastern margin of the Slave craton, are of equivalent age to the Lake Superior GIF. Notably, a ~20-m-thick magnetite-hematite oolitic iron formation is present in the middle member of the Watterson Formation (Hurwitz Group)

on the Hearne craton (Miller and Reading, 1993). The age of this oolitic unit is not well constrained, but ages of detrital zircons in the Hurwitz Group suggest that it is younger than 1.9 Ga (Davis et al., 2005). In addition, presence of iron formation in the ca. 1.88 Ga Rochford Formation developed on the eastern margin of the Wyoming craton supports synchronous deposition of iron formation on several cratons, even though this deposit is poorly dated and not granular (e.g., Frei et al., 2008).

Deposition of iron formation on the Superior craton is coincident with a peak in tonnage for VMS deposits, some of which were positioned in arcs adjacent to the craton. VMS deposits of this age are known in the hinterland to the south of the Animikie basin (Schulz and Cannon, 2007), in the Labrador Trough (Barrett et al., 1988), and in the Trans-Hudson Orogen (Syme and Bailes, 1993). Recent geochronological studies of the host metavolcanic rocks to VMS deposits in the Pembine-Wausau terrane of northern Wisconsin indicate that these deposits formed at ca. 1.875 Ga, contemporaneously with GIF of the Animikie basin (Schulz and Cannon, 2008). These data also suggest that the hydrothermal systems were likely the source of iron, consistent with earlier models (e.g., Isley, 1995). Iron-oxide exhalites are conspicuously absent at or near these deep-water VMS deposits that presumably formed under open-marine conditions. This observation is unlikely to reflect preservational bias, since slightly younger 1.84, 1.79, and 1.78 Ga Cu-rich VMS deposits that similarly formed in arc settings contain abundant hematite and magnetite exhalites, jasper, and iron formation (Slack et al., 2007; Slack and Cannon, 2009). This association points to an anoxic and ferruginous composition of deep waters in open-marine settings at ca. 1.93-1.88 Ga. Furthermore, assuming that the iron was hydrothermally derived, there must have been a crash, potentially to Archean levels, of the marine sulfate reservoir, which would have fostered iron-rich rather than sulfide-rich hydrothermal fluids (Kump and Seyfried, 2005). Again, this conclusion is based on the idea that the redox state and chemical composition of seawater-derived hydrothermal

fluids are strongly influenced by the concentration of the main oxidant in seawater—sulfate (Kump and Seyfried, 2005).

The Animikie basin contains another stratigraphic level with regionally extensive iron formation. This level is stratigraphically above the 1.85 Ga Sudbury impact ejecta layer and is older than the ca. 1.83 Ga regional metamorphic event related to the Penokean Orogeny (Cannon et al., 2010). These BIF are mineralogically and texturally different from the ca. 1.88 Ga GIF and were likely deposited in deeper-waters, below fair-weather wave base and, probably, even below storm wave base. They are developed in the: (1) Marquette Iron Range, Michigan (~60-m-thick Bijiki Iron-Formation Member of the Michigamme Slate containing siderite, chert, iron oxides, and silicates; Ojakangas, 1994, Ojakangas et al., 2001; Cannon et al., 2010); (2) Iron River-Crystal Falls Iron Ranges in Michigan (~15-m-thick chert-siderite slate of the Stambaugh Formation; James et al., 1968); and (3) Gogebic Iron Range, Wisconsin (~47-m-thick iron formation of the Tyler Formation consisting of chert and siderite; Schmidt, 1980; Cannon et al., 2008). Deposition of these BIF might be genetically linked with submarine mafic volcanism in the Animikie basin based on spatial association with, for example, the Badwater Greenstone, but this relationship has not been documented in detail. The BIF are commonly interbedded with, or overlain by, black sulfidic shales, which likely record the development of euxinic conditions in parts of the Animikie basin (e.g., Poulton et al., 2004; Poulton et al., 2010). Despite poor exposure, these iron deposits are easily traceable by magnetic anomalies. These units indicate that the conditions necessary for iron formation deposition in marine settings were re-established in the Animikie basin after 1.85 Ga, in association with mafic volcanism. Evidence for a shallow redoxcline in this case, however, is absent. Furthermore, the duration of these conditions was likely short, and the extent of iron formation deposition was probably limited.

3.4 Proterozoic age gap in Superior-type IF deposition

It is generally assumed that after ca. 1.85 Ga, Superior-type iron formation were not deposited for approximately 1.1 billion years (Isley and Abbott, 1999; Huston and Logan, 2004; Klein, 2005; Slack and Cannon, 2009). This gap is explained by a shift to fully oxic (Holland, 1984), sulfidic (Canfield, 1998), or suboxic (Slack et al., 2007; 2009) deep-ocean conditions. The earlier suggestion of oxic deep-ocean conditions after ca. 1.88 Ga (Holland, 1984) was challenged by the more recent interpretation that deep-ocean conditions were predominantly euxinic (anoxic and sulfidic) until ocean ventilation during the late Neoproterozoic or earliest Phanerozoic (e.g., Canfield, 1998; Poulton et al., 2004). This interpretation is grounded in a simple modelling approach that suggests full ocean ventilation would be difficult given most current estimates for atmospheric oxygen levels in the Middle Proterozoic.

Although there are a few instances of locally developed mid-Proterozoic euxinia (e.g., Shen et al., 2003; Brocks et al., 2005; Lyons et al., 2009), the idea of global-scale deep euxinia has recently also fallen out of favour. All available data that constrain the marine landscape in the mid-Proterozoic ocean are consistent with only locally-developed euxinic conditions along productive continental margins (e.g., in oxygen minimum zones) or in intracratonic basins (Scott et al., 2008; Poulton et al., 2010; Planavsky et al., 2011; Lyons et al., 2012; Reinhard et al., 2013). The emerging consensus is that the redox state of the deep ocean was spatially and temporally variable during the mid-Proterozoic but was generally at a low oxidation state (e.g., Planavsky et al., 2011). Poulton et al. (2010) argued that euxinic shales deposited on continental margins in oxygen-minimum zones and in intracratonic basins could have been a major sink for the hydrothermal iron flux to the mid-Proterozoic oceans and were thus responsible for the absence or scarcity of mid-Proterozoic IF. At present, this suggestion has not been quantitatively evaluated, but it predicts very high Fe content in euxinic shales during this time interval. Data in Kump and Holland (1992) do show that the average

Proterozoic shale has more Fe than the average Phanerozoic shale but less than the average Archean shale.

Large sedimentary iron deposits during this time gap (1.85-0.75 Ga) are indeed absent, but several small iron formation and iron-rich lithologies in sedimentary rock-dominated successions are known (see Bekker et al., 2010). Examples within this age group include the ca. 1.7 Ga Freedom Formation of the Lower Baraboo Series, Wisconsin, which contains banded ferruginous chert in the lower part interlayered with sideritic and kaolinitic slate, collectively ranging from 60 to 160 m thick (Weidman, 1904; Leith, 1935; Van Wyck and Norman, 2004). The broadly correlative metasedimentary succession of the Tomiko terrane in Ontario contains magnetite-chert iron formation (Easton, 2005). Additionally, the Chuanlinggou iron formation of the North China craton, a classic GIF deposit, also appears to be latest Paleoproterozoic in age (ca. 1.7 Ga; Wan et al., 2003; Dai et al., 2004). The Sherwin Formation of the Mt. Isa Superbasin, Australia also hosts classic GIF, which was deposited around 1.4 Ga (Bekker et al., 2010). A relatively large-scale mining operation based on this unit began in 2011. The iron formation in the ca. 0.8 Ga Aok Formation of the Shaler Group, Victoria Island, Northern Canada (Bekker et al., 2010), although thin stratigraphically, is mineralogically and texturally more similar to some Archean iron formations than to any Phanerozoic iron-rich unit.

Even though iron formation deposited during this time interval are spatially limited, relative to massive Neoproterozoic deposits, their existence may be significant. For example, these deposits may provide evidence for rare upwelling of hydrothermal iron from deep-water oceanic settings from ca. 1.85 to 0.8 Ga. That said, these units are still poorly studied, and we cannot rule out alternative depositional models (e.g., iron-rich groundwater, local shallow-water hydrothermal iron sources, and iron recycled from sediments deposited in inner-shelf mud belts). Between 1.85 and 0.8 Ga, open-marine, deep-water environments may, in some cases, have been sufficiently oxygenated to

oxidise and precipitate Fe(II) from hydrothermal plumes as ferric oxyhydroxides (e.g., Slack et al., 2007), while evidence for Mn(II) oxidation in the deep ocean are lacking. Although this record of the iron cycle does not provide strong quantitative constraints on the deep-ocean redox state, it questions models invoking either persistently oxic or fully sulfidic conditions throughout the deep ocean in the mid-Proterozoic. Again, in terms of time and space, a low but variable redox state in the deep ocean is most consistent with the mid-Proterozoic iron deposit record. Considering the absence of evidence for Mn(II) oxidation in the deep ocean during this time interval, and to differentiate it from the Archean deep ocean redox record, perhaps we should refer to the Middle Proterozoic ocean as a “manganiferous ocean”.

4. Iron Formations, Primary Productivity, and Atmospheric Oxygenation

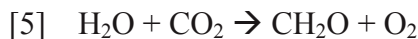
Although there is still debate about the dynamics of initial atmospheric oxygenation, herein we present a coherent model for the rise of atmospheric O₂. Underpinning this transition was the evolution of cyanobacteria and the oxygen they generated. As discussed above, several lines of evidence tentatively point to their evolution by at least 2.7 Ga (see above; Buick, 2008).

If cyanobacteria evolved by 2.7 Ga or before, the obvious question is why did it take several hundred million years for oxygen to accumulate in the atmosphere? To maintain low atmospheric oxygen levels despite O₂ production in the oceans requires that oxygen sinks must have been much larger than they are now (including solutes in seawater, volcanic gases, or crust), or the oxygen flux was greatly reduced (due to limited cyanobacterial productivity), or both (Figure 7). It is important to remember that most organic matter produced in the upper water column will be remineralised in the water column, even if there is a surge in productivity associated with the evolution of cyanobacteria. And, this relationship will likely hold even if marine sulfate levels were very low (e.g., 100 μM). Therefore, oxygen flux calculations on local or global scales need to consider the

very large offset between export and primary production. That being said, there should be an oxygen flux to the atmosphere in the Archean in the presence of cyanobacterial production, and exactly how oxygen levels were buffered at very low levels remains an unresolved question. In this regard, there are several possibilities.

First, based on the low P/Fe ratios in Archean and Paleoproterozoic IF, it was proposed that seawater at that time contained limited marine phosphorous. This, in turn, would have reduced levels of photosynthesis and carbon burial, thereby inhibiting long-term oxygen production on the early Earth (Bjerrum and Canfield, 2002). This model is based on derived partitioning coefficients (K_D) for P to ferric oxyhydroxides associated with modern hydrothermal plumes. However, because the K_D value for P sorption to ferric oxyhydroxides varies inversely with dissolved silica concentrations owing to competitive sorption of aqueous silica (Konhauser et al., 2007a), it was subsequently shown that when the evolution of the marine Si cycle is also considered, Archean phosphate concentrations would not have been limiting to cyanobacterial productivity (Konhauser et al., 2007a; Planavsky et al., 2010b). For instance, P/Fe ratios of early Phanerozoic hydrothermal jasper are similar to those of Archean IF. Indeed, phosphate concentrations may have even been elevated in the Archean, considering the evolution of marine P burial fluxes (Planavsky et al., 2010b), suggesting that if cyanobacteria were nutrient-limited, it was likely more due to a trace nutrient.

Second, reduced solutes in the oceans could have served as a buffer to the increasing amounts of O_2 produced. For instance, the oceans were rich in dissolved ferrous iron, as testified by the presence of iron formations deposited between 2.7-2.4 Ga. However, it is unclear if iron buffering alone could balance a moderate oxygen flux. It is important to note that for 1 mole of O_2 reacting with ferrous iron in solution, 4 moles of Fe^{2+} are consumed [see reactions 5-6], and thus, it is widely held that Fe(II) alone could not have been the main O_2 sink (e.g., Towe, 1994).



Others have proposed that the additional buffering capacity was provided by reduced volcanic and metamorphic gases (e.g., Kump et al., 2001); however, for these sinks to be larger in the Archean than the Proterozoic, volcanic and metamorphic gases must have been more reducing unless the O₂ production flux was smaller. Kump and Barley (2007) proposed that in the Archean volcanism was predominantly restricted to submarine settings and that volatiles released during submarine volcanism were more reducing than in subaerial settings (as they are today) because they contain more H₂, CO, CH₄ and H₂S. Following the Archean–Proterozoic transition, subaerial volcanism appears to have become more pervasive as a result of continental stabilisation. A shift from predominantly submarine to subaerial volcanism, releasing more oxidising volatiles such as H₂O, CO₂, and SO₂, would have reduced the overall sink for oxygen and led to the rise of atmospheric oxygen. Along similar lines, Gaillard et al. (2011) proposed that a decrease in the average pressure of volcanic degassing changed the oxidation state of sulfur in volcanic gases from predominantly H₂S to SO₂.

A recent twist on this story comes from the analysis of nickel concentrations (expressed as molar Ni/Fe ratios) in iron formation through time, which shows a dramatic drop in Ni availability in the oceans around 2.7–2.6 Ga (Pecoits et al., 2009; Konhauser et al., 2009). The drop in seawater Ni content after 2.7 Ga is consistent with a progressively cooling Archean mantle, whereby the volume of ultramafic melts produced by partial mantle melting and eruption of Ni-bearing ultramafic volcanic rocks (known as komatiites) decreased, and, subsequently, less Ni was dissolved into seawater. This drop in Ni availability could have had profound consequences for

microorganisms that depended on it, specifically methane-producing bacteria or methanogens (Konhauser et al., 2009). These bacteria have a unique Ni requirement for their methane-producing enzymes, and a limitation in this metal could have decreased their population in seawater. Compounding their plight, increased supply of sulfate to the oceans after about 2.5 Ga (e.g., Cameron, 1983) would have fostered competition between the starving methanogens and the increasingly abundant sulfate-reducing bacteria, the latter having a competitive edge in terms of substrate utilisation (Zahnle et al., 2006). The net result would have been the marginalisation of methanogens from the water column to anoxic and sulfate-poor sediments, where we find them today. It is thus possible that a Ni famine eventually led to a cascade of events that began with reduced methane production, the expansion of cyanobacteria into deep-water settings previously occupied by methanogens, and ultimately increased oxygenic photosynthesis that tipped the atmospheric redox balance in favour of oxygen, leading to the GOE around 2.45 Ga (Konhauser et al., 2011). At the heart of this model is the simple idea that a decreased flux of methane would lead to greater oxygen concentrations in the atmosphere even if the marine O₂ flux to the atmosphere remained constant.

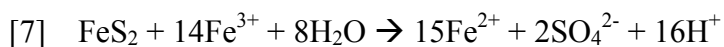
Is there any other evidence in the rock record to support a change in biological dynamics between methanogens and cyanobacteria? The answer may come from sections of Neoproterozoic shallow and deep-water sediments from the Hamersley Province that record 150 million years of Archean history. As discussed above, Eigenbrode and Freeman (2006) observed a ¹²C enrichment in the organic carbon fraction that most likely represents microbial habitats influenced by the assimilation of methane, i.e., methanotrophy. Interestingly, however, there is a ¹³C enrichment of 10‰ in kerogen in the post-2.7 Ga shallow-water facies relative to the deep-water settings, suggesting that the shallow waters became oxygenated (or oxidant-rich) as presumably cyanobacteria expanded their metabolic influence. At the same time, the deep waters still remained

a viable environment for the methanogens and methanotrophs. As populations of sulfate-reducing bacteria in the oceans increased, due to the rise of atmospheric oxygen and concomitantly higher seawater sulfate concentrations, they would have continued to marginalise the methanogens and, indirectly, methanotrophs to even greater depths in the oceans, limiting their distribution to bottom sediments. Restricting methane production largely to the sediment pile would greatly increase the chances of anaerobic methane oxidation by solid-phase ferric iron, further reducing the methane flux to the atmosphere.

By 2.5 Ga, we see evidence for oxygen accumulation in the atmosphere from the Mt. McRae Shale of Western Australia, recording the transiently oxidised conditions now widely known as the ‘whiff’ of oxygen (Anbar et al., 2007). The whiff is recorded by a spike in Mo and Re concentrations, nitrogen isotope compositions, and iron speciation data, indicating euxinic water column conditions (Anbar et al., 2007; Reinhard et al., 2009; Garvin et al., 2009). These shales lie near the middle of the 2.5 km thick Hamersley Group (dated between 2.63 and 2.45 Ga), and they directly underlie (in ascending order) the Brockman Iron Formation, Weeli Wolli Formation, Woongarra Volcanics, and the Boolgeeda Iron Formation. Scott et al. (2011) have subsequently shown that euxinic conditions could develop under an Archean anoxic atmosphere, and alternatives to the ‘whiff’ model have been proposed. For example, nitrogen isotope and redox-sensitive element signals may not require oxygen in the atmosphere, and redox cycling without oxygen and hydrothermal sources of metals to locally euxinic settings might explain these data (Bekker et al., 2009; Farquhar et al., 2011). Work remains in studies of the ‘whiff’ and for unravelling the overall pattern of atmospheric oxygenation, and there is even disagreement among the authors of this chapter.

A recent compilation of the Cr content in iron formations has contributed to our understanding of the GOE. For instance, a moderate enrichment in Cr (as expressed by its molar

Cr/Ti ratio) beginning at 2.45 Ga in the Weeli Wolli Formation, as well as the Cauê Iron Formation in Brazil, was followed by a spike in Cr enrichment in oolitic and pisolitic ironstone associated with the ca. 2.32 Ga Timeball Hill Formation (Konhauser et al., 2011). Cr enrichment in the face of muted Cr isotope fractionation at this time (Frei et al., 2009) points to a supply mechanism that involved predominately the reduced Cr(III) form (Konhauser et al., 2011). Given the insolubility of Cr(III) minerals, its mobilisation and incorporation into iron formation indicates enhanced chemical weathering at that time, most likely associated with the emergence of aerobic continental pyrite oxidation. Pyrite oxidation generates significant acidity; see reaction 7:



That acid attack would have enhanced *in-situ* dissolution of parent ultramafic/mafic material or Cr-bearing soil minerals that previously retained Cr under anoxic, but pH-neutral conditions, leading to increased continental Cr(III) supply to the oceans. Accordingly, it has been suggested that the Cr enrichment beginning ca. 2.45 Ga reflects Earth's first acid continental rock drainage, where acidity was generated with rising O₂ at unprecedented scales via the oxidation of a previously untapped terrestrial pyrite reservoir. This process continued until the easily oxidisable pyrite in the weatherable crust was diminished (Konhauser et al., 2011).

Interestingly, not all iron formation in this time window show elevated Cr enrichments (e.g., the Dales Gorge and Joffre members of the Brockman Iron Formation). Considering the low solubility of Cr(III) at marine pH, rapid reduction of Cr(VI) by aqueous Fe(II), and near instantaneous co-precipitation of Cr(III) with ferric oxyhydroxide (e.g., Fendorf, 1995), Cr dispersal would be limited upon delivery to the oceans. In this regard, proximity of the depositional site to shore played a strong role in determining which iron formation would record a continental Cr input.

Indeed, iron formation with some of the highest Cr values, such as the Cauê and Timeball Hill formations, show evidence of sediment re-working and grade into GIF, indicative of shallow-water deposition (Spier et al., 2007; Eriksson, 1973). The oolitic and pisolitic Timeball Hill Formation records the highest degree of Cr enrichment in Paleoproterozoic iron formation, which is not surprising considering its shallow-water depositional environment (pro-deltaic to offshore).

Importantly, once extensive oxidative continental weathering was initiated, it would have provided increased delivery of trace elements and sulfate to the oceans, including Mo, which would have allowed nitrogen fixers in the oceans to activate their efficient Mo-nitrogenase enzymes. With more Mo available, nitrogen fixation would have flourished, leading to increased primary productivity by photosynthetic cyanobacteria. In turn, higher net oxygen production would have further increased the terrestrial flux of dissolved Mo to the oceans. These feedback conditions would have served to alleviate the effects of nitrogen limitation and promote irreversible atmospheric oxidation (Anbar and Knoll, 2002). Turning on pyrite oxidation would have also increased the terrestrial P flux to the oceans, given the pH dependence of apatite dissolution and P solubility (Bekker and Holland, 2012).

Consistent with the above-discussed model, the oldest positive carbon isotope excursion is found in carbonates of the ca. 2.45 Ga Tongwane Formation, South Africa, which sits conformably above iron formation (Bekker et al., 2001). This small positive carbon isotope excursion is followed immediately by the onset of widespread glaciations likely related to the oxidation of atmospheric methane, an important greenhouse gas during the Archean (Bekker and Kaufman, 2007).

Intriguingly, the ability of cyanobacteria in the ocean's photic zones to remotely "mail-order" their own nutrient supply via O₂-enhanced chemical weathering may represent an unrecognised positive biological feedback (Konhauser et al., 2011). Moreover, unlike carbonic-acid driven weathering, the increased delivery of phosphorous from sulfuric acid dissolution of apatite would be

unaccompanied by increased alkalinity through bicarbonate ions. This decoupling of nutrient and bicarbonate fluxes would drive a proportional increase in organic carbon burial, a necessary condition for the generation of positive carbon isotope excursion (e.g., Aharon, 2005). The ca. 2.22-2.10 Ga Lomagundi carbon isotope excursion thus may, together with the Cr enrichment in early Paleoproterozoic iron formations, be a manifestation of acid-driven dissolution and the first sedimentary cycle of oxidative weathering (Holland, 2002; Bekker and Holland, 2012).

5. Concluding remarks

Iron formations are a defining part of the Neoproterozoic-Paleoproterozoic sedimentary record. These deposits have been studied extensively, given their importance as ore deposits, for the past 100 years. However, in the past decade alone there have been major advances in our understanding of their formation. Some of these advances have come from revisiting the role that microbial metabolic reactions likely played in their deposition and diagenesis, in phase with equally rapid progress in our understanding of microbial iron cycling more generally. Also as expected, other advances have come from application of novel isotope systems (e.g., Fe, Cr, U, Mo isotopes). With these new findings, there have been shifts from the ‘textbook view’ of iron formation genesis established during pioneering work in the 1970s and 1980s. Foremost, in contrast to the entrenched view, it is now fairly well accepted that microbial (i.e., enzymatic) Fe(II) oxidation was likely a key process in the deposition of many iron formation. Also, their deposition was unlikely to have represented typical marine sedimentation. Instead, a strong hydrothermal iron flux was often the key factor that yielded iron formation rather than more typical marine sediments. Similarly, a complex set of factors – including the evolution of hydrothermal systems – is behind their temporal distribution, rather than simply deep marine redox evolution (i.e., ocean oxygenation) as was often imagined.

Our understanding of iron formation genesis has certainly moved forward at a rapid pace, as our use of these sediments as palaeo-oceanographic archives has leaped forward in recent years. One of the most exciting advances is an increased understanding of the co-evolution of Earth surface processes with microbial metabolism during the Archean-Proterozoic transition. For example, the iron formation record has helped shape our view on the evolution of aerobic metabolisms tied to the earlier expansion of cyanobacteria throughout the surface oceans in the Archean. The emergence of an aerobic biosphere was likely brought on by an oxidative component to nutrient cycling and chemical weathering reactions, and potentially altered nutrient fluxes to the oceans. Evidence for these processes continues to be found in the trace element and isotopic signatures contained in these chemical deposits.

6. References

- Aharon, P., 2005. Redox stratification and anoxia of the early Precambrian oceans: Implications for carbon isotope excursions and oxidation events. *Precambrian Research*, 137:207-222.
- Akhmedov, A.M., 1972a. Hematite oolites in sedimentary rocks of the Pechenga complex, Materials on mineralogy of Kola Peninsula. Nauka, Leningrad, pp. 135-137, in Russian.
- Akhmedov, A.M., 1972b. Iron-rich metasedimentary rock of Pechenga complex and their genesis, Materials on geology and metallogeny of Kola peninsula, Apatity, pp. 125-131, in Russian.
- Alexander, B.W., Bau, M., Andersson, P., and Dulski, P., 2008. Continentally-derived solutes in shallow Archean seawater: Rare earth element and Nd isotope evidence in iron formation from the 2.9 Ga Pongola Supergroup, South Africa. *Geochimica et Cosmochimica Acta*, 72: 378-394.
- Allen, J.P., Olson, T.L., Oyala, P., Lee, W.J., Tufts, A.A., and Williams, J.C., 2012. Light-driven oxygen production from superoxide by Mn-binding bacterial reaction centers. *Proceedings of the National Academy of Sciences USA*, 109:2314-2318.
- Alibert, C. and McCulloch, M.T., 1993. Rare element and neodymium isotopic compositions of the banded iron-formations and associated shales from Hamersley, Western Australia. *Geochimica et Cosmochimica Acta*, 57:187-204.
- Altermann, W. and Schopf, J.W., 1995. Microfossils from the Neoproterozoic Campbell Group, Griqualand West Sequence of the Transvaal Supergroup, and their paleoenvironmental and evolutionary implications. *Precambrian Research*, 75:65-90.
- Amakawa, H., Nozakia, Y., and Masuda, A., 1996. Precise determination of variations in the $^{138}\text{Ce}/^{142}\text{Ce}$ ratios of marine ferromanganese nodules. *Chemical Geology*, 131:183-195.
- Anbar, A.D. and Holland, H.D., 1992, The photochemistry of manganese and the origin of banded iron formations. *Geochimica et Cosmochimica Acta*, 56:2595-2603.
- Anbar, A.D. and Knoll, A.H., 2002. Proterozoic ocean chemistry and evolution: A bioinorganic bridge? *Science*, 297:1137-1142.
- Anbar, A.D., Duan, Y., Lyons, T.W., Arnold, G.L., Kendall, B., Creaser, R.A., Kaufman, A.J., Gordon, G.W., Scott, C., Garvin, J., and Buick, R., 2007. A whiff of oxygen before the Great Oxidation Event? *Nature*, 317:1903-1906.
- Barghoorn, E.S. and Tyler, S.A., 1965. Microorganisms from Gunflint Chert. *Science*, 147, 563-575.
- Barley, M.E., Pickard, A.L., and Sylvester, P.J., 1997. Emplacement of a large igneous province as a possible cause of banded iron formation 2.45 billion years ago. *Nature*, 385:55-58.

- Barley, M.E., Bekker, A., and Krapež, B., 2005. Late Archean to Early Paleoproterozoic global tectonics, environmental change and the rise of atmospheric oxygen. *Earth and Planetary Science Letters*, 238:156-171.
- Barns, S.M. and Nierzwicki-Bauer, S.A., 1997. Microbial diversity in ocean, surface and subsurface environments, in: Banfield, J.F., Nealson, K.H. (Eds.), *Geomicrobiology: Interactions Between Microbes and Minerals*. Mineralogical Society of America, Washington, D.C., pp. 35-79.
- Barrett, T.J., Wares, R.P., and Fox, J.S., 1988. Two-stage hydrothermal formation of a lower Proterozoic sediment-hosted massive sulfide deposit, Northern Labrador Trough, Quebec. *Canadian Mineralogist*, 26:871-888.
- Bau, M. and Moller, P., 1993. Rare-Earth Element Systematics of the Chemically Precipitated Component in Early Precambrian Iron Formations and the Evolution of the Terrestrial Atmosphere-Hydrosphere-Lithosphere System. *Geochimica et Cosmochimica Acta*, 57:2239-2249.
- Bau, M. and Dulski, P., 1996. Distribution of yttrium and rare-earth elements in the Penge and Kuruman Iron-Formations, Transvaal Supergroup, South Africa. *Precambrian Research*, 79:37-55.
- Bau, M., Hohndorf, A., Dulski, P., and Beukes, N.J., 1997. Sources of rare-earth elements and iron in Paleoproterozoic iron-formations from the Transvaal Supergroup, South Africa: Evidence from neodymium isotopes. *Journal of Geology*, 105:121-129.
- Bau, M., Romer, R.L., Lüders, V., and Beukes, N.J., 1999. Pb, O, and C isotopes in silicified Mooidraai dolomite (Transvaal Supergroup, South Africa): Implications for the composition of Paleoproterozoic seawater and 'dating' the increase in oxygen in the Precambrian atmosphere. *Earth and Planetary Science Letters*, 174:43-57
- Baur, M.E., Hayes, J.M., Studley, S.A., and Walter, M.A., 1985. Millimeter-scale variations of stable isotope abundances in carbonates from banded iron-formations in the Hamersley Group of Western Australia. *Economic Geology*, 80:270-282.
- Beal, E.J., House, C.H., and Orphan, V.J., 2009. Manganese- and iron-dependent marine methane oxidation. *Science*, 325:184-187.
- Bjerrum, C.J. and Canfield, D.E., 2002. Ocean productivity before about 1.9 Gyr limited by phosphorous adsorption onto iron oxides. *Nature*, 417:159-162.
- Bekker, A., Kaufman, A.J., Karhu, J.A., Beukes, N.J., Swart, Q.D., Coetzee, L.L., and Eriksson, K.A., 2001. Chemostratigraphy of the Paleoproterozoic Duitschland Formation, South Africa:

- Implications for coupled climate change and carbon cycling. *American Journal of Science*, 301:261-285.
- Bekker, A., Karhu, J.A., Eriksson, K.A., and Kaufman, A.J., 2003. Chemostratigraphy of Paleoproterozoic carbonate successions of the Wyoming Craton: tectonic forcing of biogeochemical change? *Precambrian Research*, 120:279-325.
- Bekker, A., Holland, H.D., Wang, P.L., Rumble III, D., Stein, H.J., Hannah, J.L., Coetzee, L.L., and Beukes, N.J., 2004. Dating the rise of atmospheric oxygen. *Nature*, 427:117-120.
- Bekker, A. and Kaufman, A.J., 2007. Oxidative forcing of global climate change: a biogeochemical record across the oldest Paleoproterozoic ice age in North America. *Earth and Planetary Science Letters*, 258:486-499.
- Bekker, A., Barley, M.E., Fiorentini, M.L., Rouxel, O.J., Rumble, D., and Beresford, S.W., 2009. Atmospheric sulfur in Archean komatiite-hosted nickel deposits. *Science*, 326:1086-1089.
- Bekker, A., Slack, J., Planavsky, N., Krapež, B., Hofmann, A., Konhauser, K.O., and Rouxel, O.J., 2010. Iron formation: The sedimentary product of a complex interplay among mantle, tectonic, oceanic, and biospheric processes. *Economic Geology*, 105:467-508.
- Bekker, A. and Holland, H.D., 2012. Oxygen overshoot and recovery during the early Paleoproterozoic. *Earth and Planetary Science Letters*, 317:295-304.
- Berman, R.G., Sanborn-Barrie, M., Stern, R.A., and Carson, C.J., 2005. Tectonometamorphism at ca. 2.35 and 1.85 Ga in the Rae Domain, Western Churchill Province, Nunavut, Canada: Insight from structural, metamorphic, and in situ geochronologic analysis of the southwestern Committee Bay Belt. *Canadian Mineralogist*, 43:409-442.
- Berner, R.A., 1964. An idealized model of dissolved sulfate distribution in recent sediments. *Geochimica et Cosmochimica Acta*, 28:1497-1503.
- Beukes, N.J. and Klein, C., 1990. Geochemistry and sedimentology of a facies transition - from microbanded to granular iron-formation - in the early Proterozoic Transvaal Supergroup, South Africa. *Precambrian Research*, 47:99-139.
- Beukes, N.J., Klein, C., Kaufman, A.J., and Hayes, J.M., 1990. Carbonate petrography, kerogen distribution, and carbon and oxygen isotope variations in an early Proterozoic transition from limestone to iron-formation deposition, Transvaal Supergroup, South Africa. *Economic Geology*, 85:663-690.

- Beukes, N.J. and Cairncross, B., 1991. A lithostratigraphic- sedimentological reference profile for the Late Archaean Mozaan Group, Pongola Sequence: Application to sequence stratigraphy and correlation with the Witwatersrand Supergroup. *South African Journal of Geology*, 94:44–69.
- Beukes, N.J. and Gutzmer, J., 2008. Origin and paleoenvironmental significance of major iron formations at the Archean-Paleoproterozoic boundary. *Reviews in Economic Geology*, 15:5-47.
- Bjerrum, C.J. and Canfield, D.E., 2002. Ocean productivity before about 1.9 Ga ago limited by phosphorus adsorption onto iron oxides. *Nature*, 417:159-162.
- Bolhar R., Kamber B.S., Moorbath S., Fedo C.M., and Whitehouse M.J., 2004. Characterization of early Archaean chemical sediments by trace element signatures. *Earth Planetary Science Letters*, 222:43-60.
- Bosak, T., Greene, S.E., and Newman, D.K., 2007. A possible role for anoxygenic photosynthetic microbes in the formation of ancient stromatolites. *Geobiology*, 5:119-126.
- Boudreau, B., 1997. *Diagenetic Models and Their Implementation: Modelling Transport and Reactions in Aquatic Sediments*. Springer. New York. 414 pp.
- Braterman, P.S., Cairns-Smith, A.G., and Sloper, R.W., 1983. Photooxidation of hydrated Fe²⁺ - significance for banded iron formations. *Nature*, 303:163-164.
- Braun, J.-J., Pagel, M., Muller, J.-P., Bilong, P., Michard, A., and Guillet, B., 1990. Cerium anomalies in lateritic profiles. *Geochimica et Cosmochimica Acta*, 54:781-795.
- Brocks, J.J., Logan, G.A., Buick, R., and Summons, R.E., 1999. Archean molecular fossils and the early rise of eukaryotes. *Science*, 285:1033-1036.
- Brocks, J.J., Love, G.D., Summons, R.E., Knoll, A.H., Logan, G.A., and Bowden, S.A., 2005. Biomarker evidence for green and purple sulphur bacteria in a stratified Palaeoproterozoic sea. *Nature*, 437:866-70.
- Brocks, J.J., 2011. Millimeter-scale concentration gradients of hydrocarbons in Archean shales: Live-oil escape or fingerprint of contamination? *Geochimica et Cosmochimica Acta*, 75:3196-3213.
- Bronner, G. and Chauvel, J.J., 1979. Precambrian banded iron-formations of the Ijil Group (Kediat Ijil, Reguibat Shield, Mauritania). *Economic Geology*, 74:77-94.
- Buick, R., 1992. The antiquity of oxygenic photosynthesis - evidence from stromatolites in sulfate-deficient Archean lakes. *Science*, 255:74-77.
- Buick, R., 2008. When did oxygenic photosynthesis evolve? *Philosophical Transactions of the Royal Society B*, 363:2731-2743.

- Busigny, V., Lebeau, O., Ader, M., Krapež, B., Bekker, A., 2014. Nitrogen cycle in the Late Archean ferruginous ocean, *Chemical Geology*, in press.
- Byrne, R. and Sholkovitz, E., 1996. Marine chemistry and geochemistry of the lanthanides, in: Gschneider Jr., K.A., Eyring, L. (Eds.), *Handbook on the Physics and Chemistry of the Rare Earths*. Elsevier, Amsterdam, pp. 497–593.
- Cairns-Smith, A.G., 1978. Precambrian solution photochemistry, inverse segregation, and banded iron formations. *Nature*, 276:807-808.
- Cameron, E.M., 1983. Evidence from early Proterozoic anhydrite for sulfur isotopic partitioning in Precambrian oceans. *Nature*, 304:54-56.
- Canfield, D.E., 1998. A new model for Proterozoic ocean chemistry. *Nature*, 396:450-453.
- Canfield, D.E., 2006. Models of oxic respiration, denitrification and sulfate reduction in zones of coastal upwelling. *Geochimica et Cosmochimica Acta*, 70:5753–5765.
- Canfield, D.E., Ngombi-Pemba, L., Hammarlund, E.U., Bengston, S., Chaussidon, M., Gauthier-Lafaye, F., Meunier, A., Riboulleau, A., Rollion-Bard, C., Rouxel, O., Asael, D., Pierson-Wickmann, A.C., and El Albani, A., 2013. Oxygen dynamics in the aftermath of the Great Oxidation of Earth's atmosphere. *Proceedings of the National Academy of Sciences USA*, in press.
- Cannon, W.F., LaBerge, G.L., Klasner, J.S., and Schulz, K.J., 2008. The Gogebic Iron Range - A sample of the northern margin of the Penokean fold and thrust belt. U.S. Geological Survey Professional Paper, 1730, 44 p.
- Cannon, W.F., Schulz, K.J., Horton Jr, J.W., and Kring, D.A., 2010. The Sudbury impact layer in the Paleoproterozoic iron ranges of northern Michigan, USA. *Geological Society of America Bulletin*, 122:50-75.
- Carazzo, G., Jellinek, A.M., and Turchyn, A.V., 2013. The remarkable longevity of submarine plumes: Implications for the hydrothermal input of iron to the deep-ocean. *Earth and Planetary Science Letters*, 382:66-76.
- Chandler, F.W., 1980. Proterozoic redbed sequences of Canada. *Canadian Geological Survey Bulletin*, 311, 53 p.
- Chandler, F.W., 1984. Metallogenesis of an Early Proterozoic foreland sequence, eastern Hudson Bay, Canada. *Journal of the Geological Society*, 141:299-313.
- Cloud, P., 1973. Paleoecological significance of banded iron-formation. *Economic Geology*, 68:1135-1143.

- Cloud, P.E., 1965. Significance of Gunflint (Precambrian) microflora. *Science*, 148:27-35.
- Coffin, M.F. and Eldholm, O., 1994. Large igneous provinces: Crustal structure, dimensions, and external consequences. *Reviews of Geophysics*, 32:1–36.
- Condie, K.C., 1993. Chemical composition and evolution of the upper continental crust: Contrasting results from surface samples and shales. *Chemical Geology*, 104:1-37.
- Condie, K.C., Des Marais, D.J., and Abbott, D., 2001. Precambrian superplumes and supercontinents: a record in black shales, carbon isotopes and paleoclimates? *Precambrian Research*, 106:239-260.
- Corliss, J.B., Lyle, M., Dymond, J., and Crane, K., 1978. Chemistry of hydrothermal mounds near Galapagos Rift. *Earth and Planetary Science Letters*, 40:12-24.
- Crowe, S.A., Katsev, S., Leslie, K., Sturm, A., Magen, C., Nomosatryo, S., Pack, M.A., Kessler, J.D., Reeburgh, W.S., Roberts, J.A., González, L., Douglas Haffner, G., Mucci, A., Sundby, B., and Fowle, D.A., 2011. The methane cycle in ferruginous Lake Matano. *Geobiology*, 9:61-78.
- Crowe, S.A., Døssing, L.N., Beukes, N.J., Bau, M., Kruger, S.J., Frei, R., and Canfield, D.E., 2013. Atmospheric oxygenation three billion years ago. *Nature*, 501:535-538.
- Czaja, A.D., Johnson, C.M., Roden, E.E., Beard, B.L., Voegelin, A.R., Nägler, T.F., Beukes, N.J., and Wille, M., 2012. Evidence for free oxygen in the Neoproterozoic ocean based on coupled iron–molybdenum isotope fractionation. *Geochimica et Cosmochimica Acta* 86:118-137.
- Dai, Y.-D., Song, H.-M., and Shen, J.-Y., 2004, Fossil bacteria in Xuanlong iron ore deposits of Hebei Province: *Science in China, Series, D*, v. 47, p. 347–356.
- Dalton de Souza, J., Kosin, M., Melo, R.C., Oliveira, E.P., Carvalho, M.J., and Leite, C.M., 2003. Guia de excursão - geologia do segmento norte do orógeno Itabuna-Salvador-Curaçá. *Revista Brasileira de Geociências*, 33 (1-Suplemento), 27-32. [in Portuguese].
- Dauphas, N., van Zuilen, M., Wadhwa, M., Davis, A.M., Marty, B., and Janney, P.E., 2004. Clues from Fe isotope variations on the origin of Early Archean BIFs from Greenland. *Science* 306:2077-2080.
- Dauphas, N., Cates, N.L., Mojzsis, S.J., Busigny, V., 2007. Identification of chemical sedimentary protoliths using iron isotopes in the > 3750 Ma Nuvvuagittuq supracrustal belt, Canada. *Earth and Planetary Science Letters* 254, 358-376.
- Davis, W.J., Rainbird, R.H., Aspler, L.B., and Chiarenzelli, J.R., 2005. Detrital zircon geochronology of the Paleoproterozoic Hurwitz and Kiyuk groups, western Churchill Province, Nunavut. *Geological Survey of Canada Current Research-2005-F1*, 1-13.

- Derry, L.A. and Jacobsen, S.B., 1988. The Nd and Sr isotopic evolution of Proterozoic seawater. *Geophysical Research Letters*, 15:397-400.
- Derry, L.A. and Jacobsen, S.B., 1990. The chemical evolution of Precambrian seawater: Evidence from REEs in banded iron formations. *Geochimica et Cosmochimica Acta*, 54:2965-2977.
- Dorland, H.C., 1999. Paleoproterozoic laterites, red beds and ironstones of the Pretoria Group with reference to the history of atmospheric oxygen, Department of Geology. Rand Afrikaans University, Johannesburg, South Africa, p. 147.
- Easton, R.M., 2005. The Grenvillian Tomiko quartzites of Ontario: correlatives of the Baraboo quartzites of Wisconsin, the Mazatzal orogen of New Mexico, or unique? Implications for the tectonic architecture of Laurentia in the Great Lakes region. Institute on Lake Superior Geology, 51th Annual Meeting, Proceedings, Volume 51, Part 1 - Proceedings and Abstracts, 15-16.
- Edmond, J.M., Von Damm, K.L., McDuff, R.E., and Measures, C.I., 1982. Chemistry of the East Pacific Rise and their effluent dispersal. *Nature*, 297:187-191.
- Edwards, K.J., Glazer, B.T., Rouxel, O.J., Bach, W., Emerson, D., Davis, R.E, Toner, B.M., Chan, C.S., Tebo, B.M., Staudigal, H., and Moyer, C.L., 2011. Ultra-diffuse hydrothermal venting and biogenic mass Fe–Mn deposition at 5000 m off Hawaii. *ISME Journal*. <http://dx.doi.org/10.1038/ismej.2011.48>.
- Eigenbrode, J. L. and Freeman, K.H., 2006. Late Archean rise of aerobic microbial ecosystems. *Proceedings of the National Academy of Sciences USA*, 103:15759-15764.
- Eigenbrode, J. L. Freeman, K.H., and Summons, R.E., 2008. Methylhopane biomarker hydrocarbons in Hamersley Province sediments provide evidence for Neoproterozoic aerobicity. *Earth and Planetary Science Letters*, 273:323-331.
- Emerson, D., 2009. Potential for iron-reduction and iron-cycling in iron oxyhydroxide-rich microbial mats at Loihi Seamount. *Geomicrobiology Journal*, 26:639-647.
- England, G.L., Rasmussen, B., Krapež, B., and Groves, D.I., 2002. Paleoenvironmental significance of rounded pyrite in siliciclastic sequences of the Late Archean Witwatersrand Basin: oxygen-deficient atmosphere or hydrothermal alteration? *Sedimentology*, 49:1133–1156.
- Eriksson, K. A., 1973. The Timeball Hill Formation: A fossil delta. *Journal of Sedimentary Research*, 43:1046–1053.
- Eriksson, P.G., Engelbrecht, J.P., Res, M., and Harmer, R.E., 1994a. The Bushy Bend lavas, a new volcanic member of the Pretoria Group, Transvaal Sequence. *South African Journal of Geology*, 97, 1-7.

- Eriksson, P.G., Reczko, B.F.F., Merkle, R.K.W., Schreiber, U.M., Engelbrecht, J.P., Res, M., and Snyman, C.P., 1994b. Early Proterozoic black shales of the Timeball Hill Formation, South Africa: volcanogenic and palaeoenvironmental influences. *Journal of African Earth Sciences*, 18:325-337.
- Ernst, R.E. and Buchan, K.L., 2001. Large mafic magmatic events through time and links to mantle-plume heads, in: Ernst, R.E., Buchan, K.L. (Eds.), *Mantle Plume: Their identification through time*. Geological Society of America, Boulder, CO, pp. 483-575.
- Farquhar, J., Bao, H., and Thiemens, M., 2000. Atmospheric influence of Earth's earliest sulfur cycle. *Science*, 289:756-758.
- Farquhar, J., Zerkle, A.L., and Bekker, A., 2011. Geological constraints on the origin of oxygenic photosynthesis. *Photosynthesis Research*, 107:11-36.
- Fendorf, S.E., 1995. Surface reactions of chromium in soils and waters. *Geoderma*, 67:55-71.
- Fetter, A.H., Van Schmus, W.R., Santos, T.J.S., Neto, J.A.N., and Henriarthaud, M., 2000. U-Pb and Sm-Nd geochronological constraints on the crustal evolution and basement architecture of Ceará state, NW Borborema Province, NE Brazil: Implications for the existence of the Paleoproterozoic supercontinent "Atlantica". *Revista Brasileira de Geociências*, 30:102-106.
- Findlay, J.M., Parrish, R.R., Birkett, T.C., and Watanabe, D.H., 1995. U-Pb ages from the Nimish Formation and Montagnais glomeroporphyritic gabbro of the central New Quebec Orogen, Canada. *Canadian Journal of Earth Sciences*, 32:1208-1220.
- Fischer, W.W., Schröder, S., Lacassie, J.P., Beukes, N.J., Goldberg, T., Strauss, H., Horstmann, U.E., Schrag, D.P., and Knoll, A.H., 2009. Isotopic constraints on the Late Archean carbon cycle from the Transvaal Supergroup along the western margin of the Kaapvaal Craton, South Africa. *Precambrian Research*, 169:15-27.
- Fralick, P., Davis, D.W., and Kissin, S.A., 2002. The age of the Gunflint Formation, Ontario, Canada: single zircon U-Pb age determinations from reworked volcanic ash. *Canadian Journal of Earth Science*, 39:1085-1091.
- Fralick, P.W. and Pufahl, P. K., 2006. Iron formation in Neoproterozoic deltaic successions and the microbially mediated deposition of transgressive systems tracts. *Journal of Sedimentary Research*, 76:1057-1066.
- Frei, R., Dahl, P.S., Duke, E.F., Frei, K.M., Hansen, T.R., Frandsson, M.M., and Jensen, L.A., 2008. Trace element and isotopic characterization of Neoproterozoic and Paleoproterozoic iron formations in the Black Hills (South Dakota, USA): Assessment of chemical change during 2.9-

- 1.9 Ga deposition bracketing the 2.4-2.2 Ga first rise of atmospheric oxygen. *Precambrian Research*, 162:441-474.
- Frei, R., Gaucher, C., Poulton, S.W. and Canfield, D.E., 2009. Fluctuations in Precambrian atmospheric oxygenation recorded by chromium isotopes. *Nature*, 461: 250-253.
- Froehlich, P.N., Klinkhammer, G.P., Bender, M.L., Luedtke, N.A., Heath, G.R., Cullen, D., Dauphin, P., Hammond, D., Hartman, B., and Maynard, V., 1979. Early oxidation of organic matter in pelagic sediments of the eastern equatorial Atlantic: Suboxic diagenesis. *Geochimica et Cosmochimica Acta*, 43:1075-1090.
- Frost, C.D., von Blanckenburg, F., Schoenberg, R., Frost, B.R., and Swapp, S.M., 2007. Preservation of Fe isotope heterogeneities during diagenesis and metamorphism of banded iron formation. *Contributions to Mineralogy and Petrology*, 153:211-235.
- Fryer, B.J., 1976. Rare earth evidence in iron-formations for changing Precambrian oxidation states. *Geochimica et Cosmochimica Acta*, 41:361- 367.
- Gaillard, F., Scaillet, B., and Arndt, N.T., 2011. Atmospheric oxygenation caused by a change in volcanic degassing pressure. *Nature*, 478:229-233.
- Garrels, R.M., Perry, E.A., and Mackenzie, F.T., 1973. Genesis of Precambrian iron-formations and development of atmospheric oxygen. *Economic Geology*, 68:1173-1179.
- Garvin, J., Buick, R., Anbar, A.D., Arnold, G.L., and Kaufman, A.J., 2009. Isotopic evidence for an aerobic nitrogen cycle in the latest Archean. *Science*, 323:1045–1048.
- German, C.R. and Elderfield, H., 1990. Application of the C e-anomaly as a paleoredox indicator: The ground rules. *Paleoceanography*, 5:823-833.
- German, C.R., Holliday, B.P., and Elderfield, H., 1991. Redox cycling of rare earth elements in the suboxic zone of the Black Sea. *Geochimica et Cosmochimica Acta*, 55:3553-3558.
- Godfrey, L.V. and Falkowski, P.G., 2009. The cycling and redox state of nitrogen in the Archaean ocean. *Nature Geoscience*, 2:725-729.
- Gole, M.J. and Klein, C., 1981. Banded Iron-Formation through much of Precambrian time. *Journal of Geology*, 89:169-183.
- Golubic, S. and Lee, S.J., 1999. Early cyanobacterial fossil record: preservation, palaeoenvironments and identification. *European Journal of Phycology*, 34:339-348.
- Goode, A.D.T., Hall, W.D.M., and Bunting, J.A., 1983. The Nabby basin of Western Australia, in: Trendall, A.F., Morris, R.C. (Eds.), *Iron-formation: Facts and Problems*. Elsevier Science Publishers, Amsterdam, pp. 295-323.

- Goodwin, A.M., 1962. Structure, stratigraphy, an origin of iron formations, Michipicoten Area, Algoma District, Ontario, Canada. *Geological Society of America Bulletin*, 73:561-586.
- Gross, G.A., 1980. A classification of iron-formation based on depositional environments. *Canadian Mineralogists*, 18:215–222.
- Grotzinger, J.P. and Knoll, A.H., 1999. Stromatolites in Precambrian carbonates: evolutionary mileposts or environmental dipsticks. *Annual Reviews in Earth and Planetary Sciences*, 27:313-358.
- Gruner, J.W., 1922. The origin of sedimentary iron-formations: The Biwabik Formation of the Mesabi Range. *Economic Geology*, 22:407-460.
- Guo, Q., Strauss, H., Kaufman, A. J., Schröder, S., Gutzmer, J., Wing, B., Baker, M. A., Bekker, A., Kim, S.-T., and Farquhar, J., 2009, Reconstructing Earth's surface oxidation across the Archean-Proterozoic transition. *Geology*, 37:399-402.
- Hamilton, M.A., Buchan, K.L., Ernst, R.E., and Stott, G.M., 2009. Wide- spread and short-lived 1870 Ma mafic magmatism along the northern Superior Craton margin [abs.]: EOS Transactions, American Geophysical Union, 2009 Joint Assembly, Toronto, Canada, Abstract GA11A-01.
- Hannah, J.L., Bekker, A., Stein, H.J., Markey, R.J., and Holland, H.D., 2004. Primitive Os and 2316 Ma age for marine shale: Implications for Paleoproterozoic glacial events and the rise of atmospheric oxygen. *Earth and Planetary Science Letters*, 225:43-52.
- Hartlaub, R.P., Heaman, L.M., Chacko, T., Ashton, K.E., 2007. Circa 2.3 Ga magmatism of the Arrowsmith Orogeny, Uranium City Region, Western Churchill Craton, *Canadian Journal of Earth Sciences*, 115:181-195.
- Hartman, H., 1984. The Evolution of photosynthesis and microbial mats: A speculation on the banded iron formations, in: Cohen, Y., Castenholz, R.W., Halvorson, H.O. (Eds.), *Microbial mats: Stromatolites*. Alan R. Liss, New York, pp. 449-453.
- Hawley, J.E., 1926. Geology and economic possibilities of Sutton Lake area, District of Patricia. Ontario Department of Mines, Annual Report, 34, 56.
- Hayashi, T., Tanimizu, M., and Tanaka, T., 2004. Origin of negative Ce anomalies in Barberton sedimentary rocks, deduced from La–Ce and Sm–Nd isotope systematics. *Precambrian Research*, 135:345-357.
- Hayes, J.M., 1983. Geochemical evidence bearing on the origin of aerobiosis, a speculative hypothesis, in: Schopf, J.W. (Eds.), *Earth's Earliest Biosphere, its Origins and Evolution*. Princeton University Press, Princeton, pp. 291-301.

- Heaman, L.M., Machado, N., Krogh, T.E., and Weber, W., 1986. Precise U-Pb zircon ages for the Molson dyke swarm and the Fox River sill: constraints for Early Proterozoic crustal evolution in northeastern Manitoba, Canada. *Contr. Mineralogy and Petrology*, 94:82-89.
- Heaman, L.M., 1997. Global mafic volcanism at 2.45 Ga: Remnants of an ancient large igneous province? *Geology*, 25:299-302.
- Heaman, L.M., Peck, D., and Toope, K., 2009. Timing and geochemistry of 1.88 Ga Molson Igneous Events, Manitoba: Insights into the formation of a craton-scale magmatic and metallogenic province. *Precambrian Research*, 172:143-162.
- Heimann, A., Johnson, C.M., Beard, B.L., Valley, J.W., Roden, E.E., Spicuzza, M.J., and Beukes, N.J., 2010. Fe, C, and O isotope compositions of banded iron formation carbonates demonstrate a major role for dissimilatory iron reduction in ~ 2.5 Ga marine environments. *Earth and Planetary Science Letters*, 294:8-18.
- Heising, S., Richter, L., Ludwig, W., and Schink, B., 1999. *Chlorobium ferrooxidans* sp nov., a phototrophic green sulfur bacterium that oxidizes ferrous iron in co-culture with a "Geospirillum" sp strain. *Archives of Microbiology*, 172:116-124.
- Hoffman, P.F., 1987. Early Proterozoic foredeeps, foredeep magmatism, and Superior-type iron formations of the Canadian Shield, in: Kröner, A. (Ed.), *Proterozoic Lithospheric Evolution*. American Geophysical Union / Geological Society of America, Washington, DC; Boulder, CO, pp. 85-98.
- Hoffman, P.F., 2011. Birthdate for the Coronation paleocean: age of initial rifting in Wopmay orogen, Canada. *Canadian Journal of Earth Sciences*, 48:281-293.
- Hofmann, A., Bekker, A., Rouxel, O.J., Rumble, D., Master, S., 2009. Multiple sulphur and iron isotope composition of detrital pyrite in Archaean sedimentary rocks: a new tool for provenance analysis. *Earth and Planetary Science Letters*, 286:436-445.
- Holland, H.D., 1973. Oceans - possible source of iron in iron-formations. *Economic Geology*, 68:1169-1172.
- Holland, H.D., 1984. *The Chemical Evolution of the Atmosphere and Oceans* Princeton University Press, Princeton, NJ.
- Holland, H.D., 2002. Volcanic gases, black smokers, and the Great Oxidation Event. *Geochimica et Cosmochimica Acta*, 66:3811-3826.

- Holm, N.G., 1989. The $^{13}\text{C}/^{12}\text{C}$ ratios of siderite and organic matter of a modern metalliferous hydrothermal sediment and their implications for banded iron formations. *Chemical Geology*, 77:41-45.
- Hulbert, L.J., Hamilton, M.A., Horan, M.F., and Scoates, R.F.J., 2005. U-Pb zircon and Re-Os isotope geochronology of mineralized ultramafic intrusions and associated nickel ores from the Thompson nickel belt, Manitoba, Canada. *Economic Geology*, 100:29-41.
- Huston, D.L. and Logan, B.W., 2004. Barite, BIFs and bugs: evidence for the evolution of the Earth's early hydrosphere. *Earth and Planetary Science Letters*, 220:41-55.
- Isley, A.E., 1995. Hydrothermal plumes and the delivery of iron to banded iron formation. *Journal of Geology*, 103:169-185.
- Isley, A.E. and Abbott, D.H., 1999. Plume-related mafic volcanism and the deposition of banded iron formation. *Journal of Geophysical Research*, 104:15461-15477.
- Jacobsen, S.B. and Pimentel-Klose, M.R., 1988. Nd isotopic variations in Precambrian banded iron formations. *Geophysical Research Letters*, 15:393-396.
- James, H.L., 1954. Sedimentary facies of iron-formation. *Economic Geology*, 49:235-293.
- James, H.L., Dutton, C.E., Pettijohn, F.J., and Wier, K.L., 1968. *Geology and ore deposits of the Iron River-Crystal Falls district, Iron County, Michigan*. U.S. Geological Survey Professional Paper 570, 134 p.
- Johanneson, K.H., Hawkins Jr., D.L., and Cortés, A., 2006. Do Archean chemical sediments record ancient seawater rare earth element patterns? *Geochimica et Cosmochimica Acta*, 70:871-890.
- Johnson, C.M., Beard, B.L., Beukes, N.J., Klein, C., and O'Leary, J.M., 2003. Ancient geochemical cycling in the Earth as inferred from Fe isotope studies of banded iron formations from the Transvaal craton. *Contributions to Mineralogy and Petrology*, 144:523-547.
- Johnson, C.M., Beard, B.L., and Roden, E.E., 2008. The iron isotope fingerprints of redox and biogeochemical cycling in the modern and ancient Earth. *Annual Review of Earth and Planetary Sciences*, 36:457-493.
- Kappler, A. and Newman, D.K., 2004. Formation of Fe (III) minerals by Fe(II) oxidizing photoautotrophic bacteria. *Geochimica et Cosmochimica Acta*, 68:1217-1226.
- Kappler, A., Pasquero, C., Konhauser, K.O., and Newman, D.K., 2005. Deposition of banded iron formations by anoxygenic phototrophic Fe(II)-oxidizing bacteria. *Geology*, 33:865-868.
- Karhu, J.A. and Holland, H.D., 1996. Carbon isotopes and the rise of atmospheric oxygen. *Geology*, 24:867-870.

- Kasting, J. F., 1992. Models relating to Proterozoic atmospheric and ocean chemistry. In: Schopf, J. W.; Klein, C., eds. *The Proterozoic Biosphere: A Multidisciplinary Study*. New York: Cambridge University Press; pp 1185–1187.
- Kato, Y., Yamaguchi, K.E., and Ohmoto, H., 2006. Rare earth elements in Precambrian banded iron formations: Secular changes of Ce and Eu anomalies and evolution of atmospheric oxygen in: *Chemical and Biological Evolution of Early Earth: Constraints from Banded Iron-Formations*. Ohmoto, H., Kessler, S.K. (Ed.), Geological Society of America, Denver, pp. 269-289.
- Kendall, B., Reinhard, C.T., Lyons, T.W., Kaufman, A.J., Poulton, S.W., and Anbar, A.D., 2010. Pervasive oxygenation along late Archaean ocean margins. *Nature Geoscience*, 3:647-652.
- Klein, C., 2005. Some Precambrian banded iron-formations (BIFs) from around the world: Their age, geologic setting, mineralogy, metamorphism, geochemistry, and origin. *American Mineralogist*, 90:1473-1499.
- Klein, C. and Beukes, N.J., 1992. Time distribution, stratigraphy, and sedimentologic setting, and geochemistry of Precambrian iron-formation, in: Schopf, J.W., Klein, C. (Eds.), *The Proterozoic Biosphere*. Cambridge University Press, Cambridge, pp. 139–146.
- Klinkhammer, G., Elderfield, H., and Hudson, A., 1983. Rare-earth elements in seawater near hydrothermal vents. *Nature*, 305:185-188.
- Köhler, I., Konhauser, K.O., Papineau, D., Bekker, A., and Kappler, A., 2013. Biological carbon precursor to diagenetic siderite with spherical structures in iron formations. *Nature Communications*, 4:1741, DOI:10.1038/ncomms2770.
- Konhauser, K.O., Newman, D.K., and Kappler, A., 2005. The potential significance of microbial Fe(III) reduction during deposition of Precambrian banded iron formations. *Geobiology*, 3:167-177.
- Konhauser, K.O., Lalonde, S.V., Amskold, L., and Holland, H.D., 2007a. Was there really an Archean phosphate crisis? *Science*, 315:1234-1234.
- Konhauser, K.O., Amskold, L., Lalonde, S.V., Posth, N.R., Kappler, A., and Anbar, A., 2007b. Decoupling photochemical Fe(II) oxidation from shallow-water BIF deposition. *Earth and Planetary Science Letters*, 258:87-100.
- Konhauser, K.O., 2007. *Introduction to Geomicrobiology*, Blackwell, Oxford.
- Konhauser, K.O., Pecoits, E., Lalonde, S.V., Papineau, D., Nisbet, E.G., Barley, M.A., Arndt, N.T., Zahnle, K., and Kamber, B.S., 2009. Oceanic nickel depletion and a methanogen famine before the Great Oxidation Event. *Nature*, 458:750-753.

- Konhauser, K., Lalonde, S., Planavsky, N., Pecoits, E., Lyons, T., Mojzsis, S., Rouxel, O., Fralick, P., Barley, M., Kump, L., and Bekker, A., 2011. Aerobic bacterial pyrite oxidation and acid rock drainage during the Great Oxidation Event. *Nature*, 478:369–373.
- Krapež, B., Barley, M.E., and Pickard, A.L., 2003. Hydrothermal and resedimented origins of the precursor sediments to banded iron formations: sedimentological evidence from the early Palaeoproterozoic Brockman Supersequence of Western Australia. *Sedimentology*, 50:979-1011.
- Kulik, D.A. and Korzhnev, M.N., 1997. Lithological and geochemical evidence of Fe and Mn pathways during deposition of Lower Proterozoic banded iron formation in the Krivoy Rog Basin (Ukraine), in: Nicholson, K., Hein, J.R., Bühn, B., Dasgupta, S. (Eds.), *Manganese Mineralization: Geochemistry and Mineralogy of Terrestrial and Marine Deposits*. Geological Society Special Publication No. 119, pp. 43-80.
- Kump, L.R. and Holland, H.D., 1992. Iron in Precambrian rocks: Implications for the global oxygen budget of the ancient Earth. *Geochimica et Cosmochimica Acta*, 56:3217-3223.
- Kump, L.R., Barley, M.E., and Kasting, J.F., 2001. Rise of atmospheric oxygen and the “upside-down” Archean mantle. *Geochemistry, Geophysics, Geosystems*, 2, doi:10.1029/2000GC000114.
- Kump, L.R. and Seyfried, W.E., 2005. Hydrothermal Fe fluxes during the Precambrian: Effect of low oceanic sulfate concentrations and low hydrostatic pressure on the composition of black smokers. *Earth and Planetary Science Letters*, 235:654-662.
- James, H.L., 1954. Sedimentary facies of iron-formation. *Economic Geology* 49: 235-293.
- Laajoki, K. and Saikkonen, R., 1977. On the geology and geochemistry of the Precambrian iron formations. In: Väyrylänkylä, South Puolanka area, Finland. Geological Survey Finland, Bulletin, 292, 1-137.
- Leclerc, J. and Weber, F., 1980. Geology and genesis of the Moanda manganese deposits, Republic of Gabon, in: Varentsov, I.M., Grasselly, G. (Eds.), *Geology and Geochemistry of Manganese*, Stuttgart, pp. 89-109.
- Leith, A., 1935. The pre-Cambrian of the Lake Superior region, the Baraboo district, and other isolated areas in the upper Mississippi Valley. *Kansas Geological Society Guide Books* 9, 329–332.
- Leith, C.K., 1903. The Mesabi iron-bearing district of Minnesota. United State Geological Survey, Monographs, 43, 324 pp.

- Lepp, H. and Goldich, S.S., 1964. Origin of Precambrian iron formations. *Economic Geology*, 59:1025-1060.
- Li, Y.L., Konhauser, K.O., Cole, D.R., and Phelps, T.J., 2011. Mineral ecophysiological data provide growing evidence for microbial activity in banded-iron formations. *Geology*, 39:707-710.
- Li, Y-L., Konhauser, K.O., Kappler, A., and Hao, X-L., 2013. Experimental low-grade alteration of biogenic magnetite indicates microbial involvement in generation of banded iron formations. *Earth and Planetary Science Letters*, 361:229-237.
- Lovley, D.R., Kashefi, K., Vargas, M., Tor, J.M., and Blunt-Harris, E.L., 2000. Reduction of humic substances and Fe(III) by hyperthermophilic microorganisms. *Chemical Geology*, 169:289-298.
- Lupton, J.E., 1996. A far-field hydrothermal plume from the Loihi Seamount. *Science*, 272:976-979.
- Lyons, T.W., Anbar, A.D., Severmann, S., Scott, C., and Gill, B.C., 2009. Tracking euxinia in the ancient ocean: A multiproxy perspective and Proterozoic case study. *Annual Reviews of Earth and Planetary Sciences*, 37:507-534.
- Lyons, T.W., Reinhard, C.T., Love, G.D., and Xiao, S., 2012. Geobiology of the Proterozoic eon. In: A.H. Knoll, D.E. Canfield and K.O. Konhauser (Editors). *Fundamentals of Geobiology*, Blackwell Publishing, Oxford, pp. 371-402.
- Machado, N., Clark, T., David, J., and Goulet, N., 1997. U-Pb ages for magmatism and deformation in the New Quebec Orogen. *Canadian Journal of Earth Science*, 34:716-723.
- Maliva, R.G., Knoll, A.H., and Simonson, B.M., 2005. Secular change in the Precambrian silica cycle: Insights from chert petrology. *Geological Society of America Bulletin*, 117:835-845.
- Master, S., 1991. Stratigraphy, tectonic setting, and mineralization of the Early Proterozoic Magondi Supergroup, Zimbabwe: A review. *EGRU Information Circular 238*, Johannesburg.
- Master, S., Bekker, A., Hofmann, A., 2010, A review of the stratigraphy and geological setting of the Palaeoproterozoic Magondi Supergroup, Zimbabwe - type locality for the "Lomagundi" carbon isotope excursion. *Precambrian Research*, 182:254-273.
- Melezhik, V.A., Fallick, A.E., Hanski, E.J., Kump, L.R., Lepland, A., Prave, A.R., and Strauss, H., 2005. Emergence of the aerobic biosphere during the Archean-Proterozoic transition: challenges of future research today. *GSA Today*, 15:4-11.
- Miller R. G. and O’Nions R. K., 1985. Sources of Precambrian chemical and clastic sediments. *Nature*, 314:325–330.

- Miller, A.R. and Reading, K.L., 1993. Iron-formation, evaporite, and possible metallogenetic implications for the Lower Proterozoic Hurwitz Group, District of Keewatin, Northwest Territories. *Current Research, Part C; Geological Survey of Canada, Paper 93-1C*, pp. 179-185.
- Morris, R.C., 1993. Genetic modelling for banded iron-formations of the Hamersley Group, Pilbara Craton, Western Australia. *Precambrian Research*, 60:243–286.
- Morris, R.C. and Horwitz, R.C., 1983. The origin of the BIF-rich Hamersley Group of Western Australia - deposition on a platform. *Precambrian Research*, 21:273–297.
- Nealson, K. H. and Myers, C. R., 1990. Iron reduction by bacteria: A potential role in the genesis of banded iron formations. *American Journal of Science*, 290:35-45.
- Often, M., 1985. The early Proterozoic Karasjok Greenstone Belt, Norway: a preliminary description of lithology, stratigraphy and mineralization. *Norges Geologiske Undersøkelse Bulletin 403, Geology of Finnmark - A collection of papers*, 75-88.
- Ojakangas, R.W., 1983. Tidal deposits in the Early Proterozoic basin of the Lake Superior region – the Palms and the Pokegama Formations: Evidence for subtidal shelf deposition of Superior type banded iron formation. *Geological Society of America Memoirs*, 160:49-66.
- Ojakangas, R.W., 1994. Sedimentology and provenance of the Early Proterozoic Michigamme Formation and Goodrich Quartzite, Northern Michigan—Regional stratigraphic implications and suggested correlations. *U.S. Geological Survey Bulletin 1904-R:R1-R31*.
- Ojakangas, R.W., Marmo, J.S., and Heiskanen, K.I., 2001. Basin evolution of the Paleoproterozoic Karelian Supergroup of the Fennoscandian (Baltic) Shield. *Sedimentary Geology*, 141-142:255-285.
- Olson, J.M. and Blankenship, R.E., 2004. Thinking about the evolution of photosynthesis. *Photosynthesis Research*, 80:373-386.
- Paakola, J., 1971. The volcanic complex and associated manganiferous iron formation of the Porkonen-Pahtavaara area in Finnish Lapland. *Bulletin de la Commission Géologique de Finlande*, 247, 82 p.
- Papineau, D., Mojzsis, S.J., and Schmitt, A.K., 2007. Multiple sulfur isotopes from Paleoproterozoic Huronian interglacial sediments and the rise of atmospheric oxygen. *Earth and Planetary Science Letters*, 255:188-212.
- Partridge, M.A., Golding, S.D., Baublys, K.A., and Young, E., 2008. Pyrite paragenesis and multiple sulfur isotope distribution in late Archean and early Paleoproterozoic Hamersley Basin sediments. *Earth and Planetary Science Letters*, 272:41-49.

- Partin, C., Bekker, A., Planavsky, N., Scott, C.T., Gill, B.C., Li, C., Podkovyrov, V., Maslov, V., Konhauser, K.O., Lalonde, S.V., Love, G.D., Poulton, S.W., and Lyons, T.W., 2013. Large-scale fluctuations in Precambrian atmospheric and oceanic oxygen levels from the record of U in shales. *Earth and Planetary Science Letters*, 369:284-293.
- Partin, C.A., Lalonde, S.V., Planavsky, N.J., Bekker, A., Rouxel, O.J., Lyons, T.W., and Konhauser, K.O., 2014. Uranium in iron formations and the rise of atmospheric oxygen. *Chemical Geology*, proofs.
- Pavlov, A.A. and Kasting, J.F., 2002. Mass-independent fractionation of sulfur isotopes in Archean sediments: strong evidence for an anoxic Archean atmosphere. *Astrobiology*, 2:27-41.
- Pecoits, E., Gingras, M.K., Barley, M.E., Kappler, A., Posth, N.R., Konhauser, K.O., 2009. Petrography and geochemistry of the Dales Gorge banded iron formation: paragenetic sequence, source and implications for palaeo-ocean chemistry. *Precambrian Research*, 172:163-187.
- Perry, E.C., Tan, F.C., and Morey, G.B., 1973. Geology and stable isotope geochemistry of Biwabik Iron Formation, northern Minnesota. *Economic Geology*, 68:1110-1125.
- Planavsky, N., Rouxel, O., Bekker, A., Shapiro, R., Fralick, P., and Knudsen, A., 2009. Iron-oxidizing microbial ecosystems thrived in late Paleoproterozoic redox-stratified oceans. *Earth and Planetary Science Letters*, 286:230-242
- Planavsky, N., Bekker, A., Rouxel, O., Knudsen, A., and Lyons, T.W., 2010a. Rare earth element and yttrium compositions of Archean and Paleoproterozoic iron formations revisited: New perspectives on the significance and mechanisms of deposition. *Geochimica et Cosmochimica Acta*, 74:6387-6405.
- Planavsky, N., Rouxel, O., Bekker, A., Lalonde, S., Konhauser, K.O., Reinhard, C.T., and Lyons, T.W., 2010b. The evolution of the marine phosphate reservoir. *Nature*, 467:1088–1090.
- Planavsky, N.J., McGoldrick, P., Scott, C.T., Li, C., Reinhard, C.T., Kelly, A.E., Chu, X.L., Bekker, A., Love, G.D., and Lyons, T.W., 2011. Widespread iron-rich conditions in the mid-Proterozoic ocean. *Nature*, 477:448-495.
- Planavsky, N., Rouxel, O.J., Bekker, A., Hofmann, A., Little, C.T.S., and Lyons, T.W., 2012a. Iron isotope composition of some Archean and Proterozoic iron formations. *Geochimica et Cosmochimica Acta*, 80:158-169.
- Planavsky, N.J., Bekker, A., Hofmann, A., Owens, J.D., and Lyons, T.W., 2012b. Sulfur record of rising and falling marine oxygen and sulfate levels during the Lomagundi Event. *Proceedings of the National Academy USA*, 109:18300-18305.

- Posth N.R., Hegler F., Konhauser K.O., and Kappler A., 2008. Alternating Si and Fe deposition caused by temperature fluctuations in Precambrian oceans. *Nature Geoscience*, 1:703-708.
- Posth, N.R., Huelin, S., Konhauser, K.O., and Kappler, A., 2010. Size, density and composition of cell-mineral aggregates formed during anoxygenic phototrophic Fe(II) oxidation: Impact on modern and ancient environments. *Geochimica et Cosmochimica Acta*, 74:3476-3493.
- Posth N.R., Konhauser K.O., and Kappler A., 2013a. Microbiological processes in banded iron formation deposition. *Sedimentology*, in press.
- Posth, N.R., Köhler, I., Swanner, E., Schröder, C., Wellman, E., Binder, B., Konhauser, K.O., Neumann, U., Berthold, C., Nowak, M., and Kappler, A., 2013b. Simulating Precambrian banded iron formation diagenesis. *Chemical Geology*, in press.
- Poulton, S.W., Fralick, P.W., and Canfield, D.E., 2004. The transition to a sulphidic ocean ~1.84 billion years ago. *Nature*, 431:173-177.
- Poulton, S.W., Fralick, P.W., and Canfield, D.E., 2010. Spatial variability in oceanic redox structure 1.8 billion years ago. *Nature Geoscience*, 3:486-490.
- Prilutzky, R.E., Suslova, S.N., and Nalivkina, Y.B., 1992. Reconstruction of environmental conditions of early Proterozoic carbonate deposits of the Ukrainian and Baltic Shields based on isotopic studies. *Lithology and Mineral Deposits*, 5:76-88.
- Pufahl, P.K. and Fralick, P.W., 2004. Depositional controls on Palaeoproterozoic iron formation accumulation, Gogebic Range, Lake Superior region, USA. *Sedimentology*, 51:791-808.
- Rashby, S.E., Sessions, A.L., Summons, R. E., and Newman, D.K., 2007. Biosynthesis of 2-methylbacteriohopanepolyols by an anoxygenic phototroph. *Proceedings of the National Academy of Sciences USA*, 104:15099-15104.
- Rasmussen, B. and Buick, R., 1999. Redox state of the Archean atmosphere: Evidence from detrital heavy metals in ca. 3250-2750 Ma sandstones from the Pilbara Craton, Australia. *Geology*, 27:115-118.
- Rasmussen, B., Fletcher, I.R., Brocks, J.J., and Kilburn, M.R., 2008. Reassessing the first appearance of eukaryotes and cyanobacteria. *Nature*, 455:1101-1105.
- Rasmussen, B., Fletcher, I.R., Bekker, A., Muhling, J.R., Gregory, C.J., and Thorne, A.M., 2012. Deposition of 1.88-billion-year-old iron formations as a consequence of rapid crustal growth. *Nature*, 484:498-501.
- Reinhard, C.T., Raiswell, R., Scott, C., Anbar, A.D., and Lyons, T.W. 2009. A Late Archean sulfidic sea stimulated by early oxidative weathering of the continents. *Science*, 326:713-716.

- Reinhard, C.T., Planavsky, N.J., Robbins, L.J., Partin, C., Gill, B.C., Lalonde, S.V., Bekker, A., Konhauser, K.O., and Lyons, T.W., 2013. Proterozoic ocean redox and biogeochemical stasis. *Proceedings of the National Academy of Sciences USA*, 110:5357-5362.
- Ricketts, B.D., Ware, M.J., and Donaldson, J.A., 1982. Volcaniclastic rocks and volcaniclastic facies in the middle Precambrian (Aphebian) Belcher Group, Northwest Territories, Canada. *Canadian Journal of Earth Sciences*, 19:1275-1294.
- Ridgwell, A. and Zeebe, R.E., 2005. The role of the global carbonate cycle in the regulation and evolution of the Earth system. *Earth and Planetary Science Letters*, 234:299-315.
- Roscoe, S.M., Gandhi, S.S., Charbonneau, B.W., Maurice, Y.T., and Gibb, R.A., 1987. Mineral Resource Assessment of the Area in the East Arm (Great Slave Lake) and Artillery Lake region, N.W.T. Proposed as a National Park. Geological Survey of Canada, Open File 1434, 92 pp.
- Rouxel, O.J., Bekker, A., and Edwards, K.J., 2005. Iron isotope constraints on the Archean and Paleoproterozoic ocean redox state. *Science*, 307:1088-1091.
- Roscoe, S. M., 1969. Huronian rocks and uraniferous conglomerates in the Canadian Shield. Geological Survey of Canada Paper 68-40, 205 p.
- Rye, R. and Holland, H.D., 1998. Paleosols and the evolution of atmospheric oxygen: A critical review. *American Journal of Science*, 298:621-672.
- Saito, M.A., Noble, A.E., Tagliabue, A., Goepfert, T.J., Lamborg, C.H., and Jenkins, W.J., 2013. Slow-spreading submarine ridges in the South Atlantic as a significant oceanic iron source. *Nature Geoscience*, 6:775-779.
- Schidlowski, M., Eichmann, R., and Junge, C.E., 1976. Carbon isotope geochemistry of the Precambrian Lomagundi carbonate province, Rhodesia. *Geochimica et Cosmochimica Acta*, 40:449-455.
- Schmidt, R.G., 1980. The Marquette Range Supergroup in the Gogebic iron district, Michigan and Wisconsin. U.S. Geological Survey Bulletin 1460, 96 p.
- Schneider, D.A., Bickford, M.E., Cannon, W.F., Schulz, K.J., and Hamilton, M.A., 2002. Age of volcanic rocks and syndepositional iron formations, Marquette Range Supergroup: Implications for the tectonic setting of Paleoproterozoic iron formations of the Lake Superior region. *Canadian Journal of Earth Sciences*, 39:999-1012.
- Schneiderhan, E.A., Gutzmer, J., Strauss, H., Mezger, K., and Beukes, N.J., 2006. The chemostratigraphy of a Paleoproterozoic MnFe- and BIF succession - the Voëlwater Subgroup of

- the Transvaal Supergroup in Griqualand West, South Africa. *South African Journal of Geology*, 109:63-80.
- Schröder, S., Bekker, A., Beukes, N.J., Strauss, H., and van Niekerk, H.S., 2008. Rise in seawater sulphate concentration associated with the Paleoproterozoic positive carbon isotope excursion: evidence from sulphate evaporites in the similar to 2.2-2.1 Gyr shallow-marine Lucknow Formation, South Africa. *Terra Nova*, 2:108-117.
- Schulz, K.J. and Cannon, W.F., 2007. The Penokean orogeny in the lake superior region. *Precambrian Research*, 157:4-25.
- Schulz, K.J. and Cannon, W.F., 2008. Synchronous deposition of Paleoproterozoic Superior-type banded iron-formations and volcanogenic massive sulfides in the Lake Superior region: Implications for the tectonic evolution of the Penokeon orogen [abs.]. *Geological Society of America Abstracts with Programs*, 40, 385.
- Schweigart, H., 1965. Genesis of the iron ores of the Pretoria Series, South Africa. *Economic Geology*, 60:269-298.
- Scott, C., Lyons, T.W., Bekker, A., Shen, Y., Poulton, S., Chu, X., and Anbar, A., 2008. Tracing the stepwise oxygenation of the Proterozoic biosphere. *Nature*, 452:456-459.
- Scott, C., Bekker, A., Reinhard, C.T., Schnetger, B., Krapež, B., Rumble III, D., and Lyons, T.W., 2011. Late Archean euxinic conditions before the rise of atmospheric oxygen. *Geology*, 39:119-122.
- Severmann S., Lyons T. W., Anbar A., McManus J., and Gordon G., 2008. Modern iron isotope perspective on the benthic iron shuttle and the redox evolution of ancient oceans. *Geology*, 36:487-490.
- Shen, Y., Knoll, A.H., and Walter, M.R., 2003. Evidence for low sulphate and anoxia in a mid-Proterozoic marine basin. *Nature*, 423:632-35.
- Shimizu, H., Umemoto, N., Masuda, A., and Appel, P.W.U., 1990. Sources of iron formations in the Archean Isua and Malene supracrustals, West Greenland: Evidence from La-Ce and Sm- Nd isotopic data and REE abundances. *Geochimica et Cosmochimica Acta*, 54:1147-1154.
- Shimizu, H., Amano, M., and Masuda, A., 1991. La-Ce and Sm-Nd systematics of siliceous sedimentary rocks: A clue to marine environment in their deposition. *Geology*, 19:369-371.
- Siever, R., 1992. The silica cycle in the Precambrian. *Geochimica et Cosmochimica Acta*, 56:3265-3272.

- Simonson, B.M., 1985. Sedimentology of cherts in the early Proterozoic Wishart Formation, Quebec-Newfoundland, Canada. *Sedimentology*, 32:23-40.
- Simonson, B.M., 2003. Origin and evolution of large Precambrian iron formations, in: Chan, M.A., Archer, A.W. (Eds.), *Extreme Depositional Environments: Mega End Members in Geologic Time*. Geological Society of America Special Paper 370, Boulder, CO, pp. 231-244.
- Simonson, B.M. and Goode, A.D.T., 1989. First discovery of ferruginous chert arenites in the early Precambrian Hamersley Group of Western Australia. *Geology*, 17:269-272.
- Simonson, B.M. and Hassler, S.W., 1996. Was the deposition of large Precambrian Iron Formations linked to major marine transgressions? *Journal of Geology*, 104:665-676.
- Slack, J.F., Grenne, T., Bekker, A., Rouxel, O.J., and Lindberg, P.A., 2007. Suboxic deep seawater in the late Paleoproterozoic: Evidence from hematitic chert and iron formation related to seafloor-hydrothermal sulfide deposits, central Arizona, USA. *Earth and Planetary Science Letters*, 255:243-256.
- Slack, J.F. and Cannon, W.F., 2009. Extraterrestrial demise of banded iron formations 1.85 billion years ago. *Geology*, 37:1011-1014.
- Slack, J.F., Grenne, T., and Bekker, A., 2009. Seafloor-hydrothermal Si-Fe-Mn exhalites in the Pecos greenstone belt, New Mexico, and the redox state of ca. 1720 Ma deep seawater. *Geosphere*, 5:302-314.
- Søgaard, E.G., Medenwaldt, R., and Abraham-Peskir, J.V., 2000. Conditions and rates of biotic and abiotic iron precipitation in selected Danish freshwater plants and microscopic analysis of precipitate morphology. *Water Research*, 34:2675-2682.
- Spier, C.A., de Oliveira, S.M.B., Sial, A.N., and Rios, F.J., 2007. Geochemistry and genesis of the banded iron formations of the Cauê Formation, Quadrilátero Ferrífero, Minas Gerais, Brazil. *Precambrian Research*, 152:170-206.
- Sreenivas, B. and Murakami, T., 2005. Emerging views on the evolution of atmospheric oxygen during the Precambrian. *Journal of Mineralogical and Petrological Sciences*, 100:184-201.
- Stott, G.M., Hamilton, M.A., and Kamo, S.L., 2010. Archean granitoid geochronology and interpretations, Hudson Bay Lowland; in *Summary of Field Work and Other Activities 2010*. Ontario Geological Survey, Open File Report, 6260, 21-27.
- Straub, K.L., Rainey, F.A., and Widdel, F., 1999. *Rhodovulum iodosum* sp. nov., and *Rhodovulum robiginosum* sp. nov., two new marine phototrophic ferrous-iron-oxidizing purple bacteria. *International Journal of Systematic Bacteriology*, 49:729-735.

- Stüken, E.E., Catling, D.C., and Buick, R., 2012. Contributions to late Archaean sulphur cycling by life on land. *Nature Geoscience*, 5:722-725.
- Summons, R.E., Jahnke, L.L., Hope, J.M., and Logan, G.A., 1999. 2-Methylhopanoids as biomarkers for cyanobacterial oxygenic photosynthesis. *Nature*, 400:554-557.
- Sumner, D.Y., 1997. Carbonate precipitation and oxygen stratification in Late Archean seawater as deduced from facies and stratigraphy of the Gamohaam and Frisco formations, Transvaal Supergroup, South Africa. *American Journal of Science*, 297:455-487.
- Syme, E.C. and Bailes, A.H., 1993. Stratigraphic and tectonic setting of Early Proterozoic volcanogenic massive sulfide deposits, Flin Flon, Manitoba. *Canadian Journal of Earth Sciences*, 88:566-589.
- Szpunar, M., Hand, M., Barovich, K., Jagodzinski, E., and Belousova, E., 2011. Isotopic and geochemical constraints on the Paleoproterozoic Hutchison Group, southern Australia: Implications for Paleoproterozoic continental reconstructions. *Precambrian Research*, 187:99-126.
- Tamaura, Y., Yoshida, T., and Katsura, T., 1984. The synthesis of green rust II($\text{Fe}^{\text{II}}\text{1-Fe}^{\text{II}}\text{2}$) and its spontaneous transformation into Fe_3O_4 . *Bulletin of the Chemical Society of Japan*, 57:2411-2416.
- Tanaka, T.S., H. Kawata, Y., and Masuda, A., 1982. Combined La–Ce and Sm–Nd isotope systematics in petrogenetic studies. *Nature*, 327:113 - 117.
- Thomazo, C., Ader, M., and Philippot, P., 2011. Extreme ^{15}N -enrichments in 2.72-Gyr-old sediments: evidence for a turning point in the nitrogen cycle. *Geobiology* 9: 107-120.
- Towe, K.M., 1994. Earth's earliest atmosphere: Constraints and opportunities for early evolution In: Bengtson, S. (Editor), *Early Life on Earth*. Columbia University Press, New York, pp. 36-47.
- Trendall, A. and Blockley, J., 1970. The iron formations of the Precambrian Hamersley Group, Western Australia with special reference to the associated crocidolite. *Western Australia Geological Survey Bulletin* 119.
- Trendall, A.F., 2002. The significance of iron-formation in the Precambrian stratigraphic record. *International Association of Sedimentologists Special Publications*, 33:33–66.
- Tsikos, H., Beukes, N.J., Moore, J.M., and Harris, C., 2003. Deposition, diagenesis, and secondary enrichment of metals in the Paleoproterozoic Hotazel iron Formation, Kalahari manganese field, South Africa. *Economic Geology*, 98:1449-1462.

- Tsikos, H. and Moore, J.M., 1997. Petrography and geochemistry of the Paleoproterozoic Hotazel Iron-Formation, Kalahari Manganese Field, South Africa: Implications for Precambrian Manganese Metallogenesis. *Economic Geology*, 92:87-97.
- Tyler, S.A. and Barghoorn, E.S., 1954. Occurrence of structurally preserved plants in Pre-Cambrian rocks of the Canadian Shield. *Science*, 119: 606-608.
- Valeton, I., Schumann, A., Vinx, R., and Wieneke, M., 1997. Supergene alteration since the upper cretaceous on alkaline igneous and metasomatic rocks of the Poços de Caldas ring complex, Minas Gerais, Brazil. *Analytical Geochemistry*, 12:133-154.
- Van Wyck, N. and Norman, M., 2004. Detrital zircon ages from early Proterozoic quartzites, Wisconsin, support rapid weathering and deposition of mature quartz arenites. *Journal of Geology*, 112:305-315.
- Vargas, M., Kashefi, K., Blunt-Harris, E.L., and Lovely, D.R., 1998. Microbiological evidence for Fe(III) reduction on early Earth. *Nature*, 395:65-67.
- Waldbauer, J.R., Newman, D.K., Summons, R.E., 2011. Microaerobic steroid biosynthesis and the molecular fossil record of Archean life, *Proceedings of the National Academy of Sciences USA*, 108, 13409-13414.
- Walker, J.C.G., 1984. Suboxic diagenesis in banded iron formations. *Nature*, 309:340-342.
- Wan, Y.-S., Zhang, Q.-D., and Song, T.-R., 2003. SHRIMP ages of detrital zircons from the Changcheng System in the Ming Tombs area, Beijing: Constraints on the protolith nature and maximum depositional age of the Mesoproterozoic cover of the North China craton. *Chinese Science Bulletin*, 48:2500–2506.
- Weidman, S., 1904. The Baraboo iron-bearing district of Wisconsin. *Wisconsin Geological and Natural History Survey Bulletin*, 13.
- Widdel, F., Schnell, S., Heising, S., Ehrenreich, A., Assmus, B., and Schink, B., 1993. Ferrous iron oxidation by anoxygenic phototrophic bacteria. *Nature*, 362:834-836.
- Williford, K.H., Van Kranendonk, M.J., Ushikubo, T., Kozdon, R., and Valley, J.W., 2011. Constraining atmospheric oxygen and seawater sulfate concentrations during Paleoproterozoic glaciation: In situ sulfur three-isotope microanalysis of pyrite from the Turee Creek Group, Western Australia. *Geochimica et Cosmochimica Acta*, 75:5686-5705.
- Woese, C.R., 1987. Bacterial evolution. *Microbiology Reviews*, 51:221-271.
- Xiong J., 2006. Photosynthesis: What color was its origin? *Genome Biology*, 7:245.1-245.5.

Yang, W.H., Weber, K.A., and Silver, W.L., 2012. Nitrogen loss from soil through anaerobic ammonium oxidation coupled to iron reduction. *Nature Geosciences*, 5:538-541.

Zahnle, K.J., Claire, M., and Catling, D., 2006. The loss of mass-independent fractionation in sulfur due to a Paleoproterozoic collapse of atmospheric methane. *Geobiology*, 4:271-283.

Zegeye, A., Bonneville, S., Benning, L.G., Sturm, A., Fowle, D.A., Jones, C., Canfield, D.E., Ruby, C., MacLean, L.C., Nomosatryo, S., Crowe, S.A., and Poulton, S.W., 2012. Green rust formation controls nutrient availability in a ferruginous water column. *Geology*, 40:599-602.

Figure Captions

Figure 1 – Representative images of banded and granular iron formations. (A) Mesobanding in the ca. 2.47 Ga Dales Gorge Member BIF, Brockman Iron Formation of Western Australia. (B) Overview of the Dales Gorge Member. (C) ca. 2.32 Ga GIF of the Timeball Hill Formation of South Africa. (D) Thin section of the ca. 1.88 Ga GIF of the Frere Formation, Earraheedy basin, Western Australia showing hematitic granules with chert cement.

Figure 2 – Mechanisms of Fe(II) oxidation in the Precambrian oceans. Two biologically controlled mechanisms are envisioned: (1) reaction of cyanobacterially-generated O_2 with dissolved Fe(II), and/or (2) direct oxidation via Fe(II)-based anoxygenic photosynthesis (photoferrotrophy). The Fe(II) was sourced from deep-sea hydrothermal systems, while the Fe(III) formed in the photic zone was precipitated as ferrihydrite, $Fe(OH)_3$, and deposited onto the seafloor as a precursor sediment for iron formation. Some of ferrihydrite was later reduced either through direct bacterial Fe(III) reduction by dissimilatory iron-reducing bacteria (DIR) utilising organic carbon or through a potential metabolic coupling of Fe(III) reduction and methane oxidation (e.g., Konhauser et al., 2005).

Figure 3 – Calculated thickness of a community of photoferrotrophs required to completely oxidise upwelling, Fe(II)-rich, hydrothermal waters with iron concentrations of (A) 500 μM and (B) 100 μM , at different rates of Fe(II) oxidation. Unless noted, advection and eddy-diffusion Fe supply rates are summed, with eddy-diffusion held constant at 0.1 cm^2/sec in all cases (cf., Kappler et al., 2005). Modelled advection rates are consistent with low and high annual averages for upwelling regimes on continental margins. An eddy-diffusivity value of 0.1 cm^2/sec is also shown on each plot. Dashed lines indicate the photoferrotrophic layer thickness required for Fe(II) oxidation at rates of 1.4×10^{-4} , 1.4×10^{-5} , and 1.4×10^{-6} M/day, with 1.4×10^{-5} M/day representing a conservative estimate as determined experimentally by Kappler et al. (2005). The thickness of the photoferrotrophic layer increases dramatically with low Fe(II) oxidation rates when both advection and eddy-diffusional Fe transport are considered as opposed to solely eddy-diffusional transport. At the conservatively estimated Fe(II) oxidation rate for the upwelling waters with 500 μM Fe concentration, a photoferrotrophic layer thicknesses of 17.6 and 5.6 meters are required when solely considering diffusion at rates of 1 cm^2/sec (not shown) and 0.1 cm^2/s , respectively. These

thicknesses are distinctly different than the >100 m required when both advection at 5 m/day and diffusion at $0.1 \text{ cm}^2/\text{sec}$ are considered for the same Fe concentrations in the upwelling waters. The more realistic layer thickness of ~35 m is required for an Fe(II) oxidation rate of $1.4 \times 10^{-5} \text{ M/day}$ and advection rate and eddy-diffusivity of 5 m/day and $0.1 \text{ cm}^2/\text{s}$ at $100 \text{ }\mu\text{M}$ Fe concentration in the upwelling waters.

Figure 4 – Comparison of (A) typical sediment pore-water profile during early diagenesis in a modern continental marine setting (e.g., Froelich et al., 1979; modified from Konhauser, 2007). (B) Plausible Archean pore-water profile during early diagenesis where the minerals on the right hand side are the dominant controls on pore-water Fe speciation. As shown in Figure 2, the delivery of $\text{Fe}(\text{OH})_3$ to the sediment is controlled by O_2 concentrations and/or the metabolism of photoferrotrophic bacteria.

Figure 5 – Calculated $\delta^{13}\text{C}_{\text{DIC}}$ for sediments dominated by anaerobic organic matter remineralisation. Unless noted in the legend, sediment and water column parameters are for the Santa Barbara basin from Berner (1964). Water column DIC concentration is taken from modern continental margin values and sedimentation rate and organic matter concentrations are varied at ranges typical of continental margin settings. A DIC concentration of 10 times the modern one is used as an estimate for the Archean oceans. (A) $\delta^{13}\text{C}_{\text{DIC}}$ vertical pore-water profiles for the modern Santa Barbara basin conditions compared with modelled Archean settings with 10x DIC and various organic matter fluxes. (B) $\delta^{13}\text{C}_{\text{DIC}}$ vertical pore-water profiles for modelled Archean settings with DIC 10x that in the modern seawater showing effect of variations in the sum of sedimentation and compaction (ω) from that in the modern Santa Barbara basin. (C) Effect of variations in ω , at DIC 10x that of modern seawater and labile organic matter load at 0.5x that of the modern Santa Barbara basin, on $\delta^{13}\text{C}_{\text{DIC}}$ vertical pore-water profiles for modelled Archean settings. (D) Effect of variations in ω , at DIC 10x that of modern seawater and labile organic matter load at 0.1x that of the modern Santa Barbara basin, on $\delta^{13}\text{C}_{\text{DIC}}$ vertical pore-water profiles for modelled Archean settings.

Figure 6 – Model for the evolution of ocean redox structure based on REE patterns in well-preserved iron formations. Mn(IV)-poor iron formations are likely to record seawater REE patterns. Similar to modern redox-stratified basins (A), the REE + Y pattern of late Paleoproterozoic iron formation (B) records evidence for a shuttle of metal and Ce oxides from oxic shallow seawater

across the redoxcline. Mn(IV)-hydroxide dissolution in anoxic water column lowers the Y/Ho ratios, raises the light to heavy REE ratios, and increases the Ce concentration relative to neighboring REE (La and Pr). In contrast, Archean iron formations do not display REE + Y pattern indicative of a strong oxide shuttle (C), which implies a lack of significant Mn-cycling across a redoxcline in many Archean iron formation-bearing basins. The lack of discrete redoxcline points toward microbial Fe(II) oxidation, rather than a direct reaction of Fe(II) with O₂. Modified from Planavsky et al. (2010a).

Figure 7 – Model of various sinks for biologically produced O₂ prior to the Great Oxidation Event. These might have included: (i) reactions with various reduced gases and solutes sourced from submarine hydrothermal systems, (ii) reaction with biogenic methane produced by methanogens growing in the bottom sediments and water column, and (iii) consumption via aerobic respiration.